DEI SUB NUMINE VIGET

PRINCETON UNIVERSITY

DEPARTMENT OF
AEROSPACE AND MECHANICAL SCIENCES

NATIONAL AERONAUTICS AND SPACE ADMINISTRATION
Office of Space Science and Applications
Launch Vehicle and Propulsion Programs Division
Contract NSR 31-001-078

AEROSPACE SYSTEMS and MISSION ANALYSIS RESEARCH

Solar Electric Space Mission Analysis

Final Report

AMS Report No. 843

Prepared by:
P. M. Lion
Assistant Professor

M. Handelsman
Senior Research Scientist

and
J. P. Layton
Senior Research Engineer

Approved by:
J. P. Layton
Research Leader

15 January 1969

Aerospace Systems and Mission Analysis Research (ASMAR) Program
Department of Aerospace and Mechanical Sciences
School of Engineering and Applied Science
PRINCETON UNIVERSITY

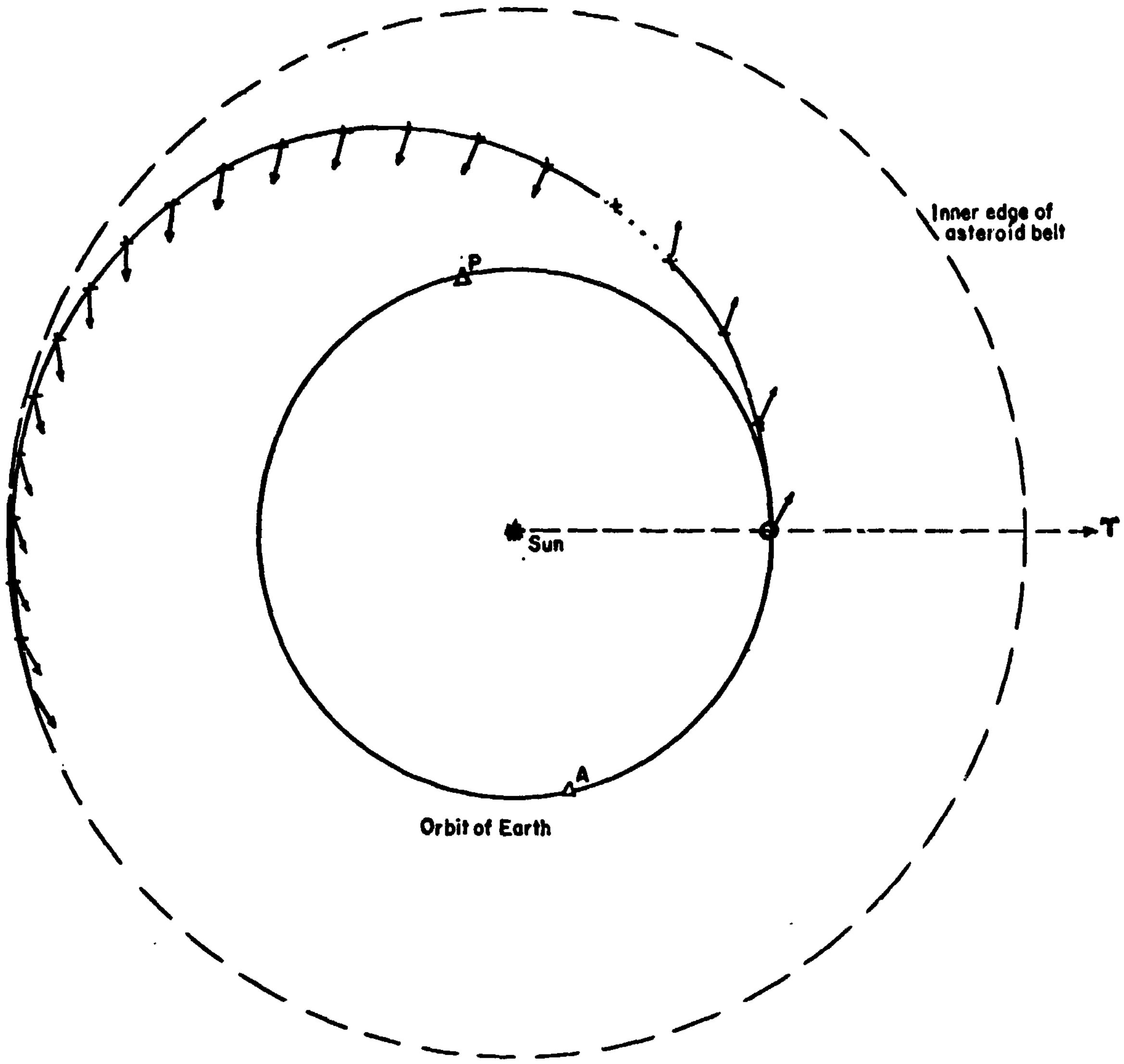

Arrows show
Thrust Direction
at 20 day intervals

Optimum Heliocentric Trajectory for a 2 AU Asteroid Rendezvous
Using a Solar Electric Propelled Spacecraft

Effective Jet Velocity = 50.0×10^{3} m s^{-1}

Initial Acceleration = 5.18×10^{-4} m s^{-2}

Flight Time = 400 days

FRONTISPIECE

SUMMARY

Preliminary mission analyses for solar powered, electric rocket propelled spacecraft on Mars orbiter, Jupiter flyby and asteroid belt exploration, trajectories were undertaken within the Aerospace Systems and Mission Analysis Research (ASMAR) Program at Princeton University.

Mars orbiter trajectories in the years 1971, 1973, 1975, 1977 and 1979 as analysed by the Hughes Aircraft Company were checked approximately using an ASMAR modification of the ITEM interplanetary trajectory computer program.

Another ASMAR computer program, Gordon 1, was used to optimize solar electric propelled Jupiter flyby trajectories which identified several trajectory modes and gave an understanding of the sensitivities to launch vehicle and propulsion technology.

Preliminary analyses of asteroid belt exploration missions, especially rendezvous trajectories with advanced technology, indicate an interesting and possibly important application of solar electric propulsion for various asteroid, planetoid and cometary missions.

ACKNOWLEDGEMENTS

This research was supported from Headquarters, National Aeronautics and Space Administration under Contract NSR 31-001-078 during the period 1 April 1966 through 30 September 1967. Mr. J. W. Haughey, Launch Vehicle and Propulsion Programs Division, Office of Space Science and Applications, and Mr. J. Mullin, Electric Propulsion Division, Office of Advanced Research Technology were the technical monitors. Thanks are extended to them for the excellent working relationships and to Mr. J. W. Stearns, Assistant Manager, Propulsion Research and Advanced Concepts and others at the Jet Propulsion Laboratory as well as to all others associated with the ASMAR Program in this endeavor.

CONTENTS

FIGURES

FIGURES (Continued)

TABLES

I. INTRODUCTION

In the fall of 1965 a representative of the Office of Advanced Research and Technology, NASA Headquarters solicited the help of the ASMAR Program in carrying out some trajectory analyses for solar electric propelled spacecraft which certain developments in solar array technology appeared to make practicable. Studies had been undertaken by several industrial concerns under contract to the Jet Propulsion Laboratory, and the ASMAR Program work was to be coordinated with this effort. A new contract, NSR 31-001-078 was awarded to support the solar electric mission analysis and the work was directed by Mr. J. Mullin of OART and Mr. J. W. Haughey of the Launch Vehicles and Propulsion Programs Division, Office of Space Science and Applications, NASA Headquarters, who was also monitor of the ASMAR Basic Program under Contract NASr-231.

ASMAR Program contact at the Jet Propulsion Laboratory was Mr. J. W. Stearns, Assistant Manager, Propulsion Research and Advanced Concepts Section; and a doctoral candidate in the ASMAR Program, Mr. G. A. Hazelrigg, Jr., was assigned to JPL for the period February-September 1966 to engage in the work there on computer analyses and programming and provide close liaison. Work at Princeton was carried out, under the overall leadership of Mr. J. P. Layton, by Drs. P. M. Lion, M. Handelsman and C. N. Gordon with programming assistance provided by Analytical Mechanics Associates, Incorporated representatives, especially Mr. J. H. Campbell.

Having made a timely contribution and completed a certain body of work that approximated the undertaking initially accepted plus some preliminary asteroid belt mission analyses, the effort by the ASMAR Program under contract NSR 31-001-078 was terminated on 30 September 1967; however, a continuing interest in and capability for trajectory and mission analysis witn solar electric propulsion will be maintained under the ASMAR Basic Program.

II. MARS ORBITER CHECK

A. Trajectory Check of Solar Electric Propelled Mars Orbiters - 1971, 1973, 1975, 1977 and 1979

Hughes Aircraft Company, under contract to the Jet Propulsion Laboratory, produced an extensive study of solar-electric propelled Mars orbiter and Jupiter flyby missions.[(1)*] Their trajectory results for the Mars orbiter contained certain optimizations, allowed for spacecraft limitations and for planetary perturbations. At the request of NASA Headquarters, a modified ITEM program (described below) was used by the ASMAR Group at Princeton to provide a check on the Hughes' results for the Mars orbiter. The preliminary results-shown on Tables[**] 1 through 5 and Figures[**] 1 through 5 yield a substantial check of the Hughes data. However, Hughes was unable to supply all the necessary input data in sufficient detail for a definitive check. Thus, the differences shown in the above results could not be refined and the attempt to obtain a better check was abandoned.

B. The Modified ITEM Program

To check the Hughes' results the ASMAR Group undertook a general rewrite of the ITEM Computer program which was obtained from Goddard Space Flight Center.

The ITEM program is a multi-body trajectory program using the Encke method of integration. Changes incorporated in this program by the ASMAR Group can be divided into (a) changes to increase flexibility in the number and type of problem which can be handled by this program and (b) changes to improve the efficiency of the computational procedures used.

---

*Superscript numbers in parentheses indicate References listed at the end of the report.

**Tables and Figures appear following the first page of text on which they are mentioned.

TABLE I

Solar Electric Propelled Mars Orbiter 1971

	Calendar Date	Julian Date
Leave Earth sphere of influence, T_o (t 0 hrs)	May 8, 1971	2441080.438
Vis-Viva Energy, C_3 = 4.284250 $km^2 s^{-2}$		
Arrive near Mars, T_f (t = 230 days + 3 hrs)	Dec 25, 1971	2441310.563
Transfer Angle = 172.888°		

	T_o		T_f			
	Earth Ephemeris	Hughes	Mars Ephemeris	Hughes	Mod. ITEM	Δ(MI-H)
X,AU	-.68351475	-.67969491	1.0972198	1.0966328	1.0834762	-.0131566
Y,AU	-.74280646	-.74666393	.95511574	.95591247	.96126080	+.0053483
Z,AU	.000042125583	-.00278906	-.00658942	.00333529	.00255740	-.0007779
$\dot{X}$,EMOS	.71937913	.76916774	-.50211714	-	-.46638744	-
$\dot{Y}$,EMOS	-.68040780	-.72639255	.68244455	-	.63241905	-
$\dot{Z}$,EMOS	.000041832549	-.03492263	.02666489	-.00174490	-.02570829	-.0239634
S/C Mass, kgm	2514.3			-	2325.7	-
Ratio S/C Mass @ T_f/T_o				-	.9250	-
Approach Speed to Mars, km s^{-1}				1.961	2.405	+.444

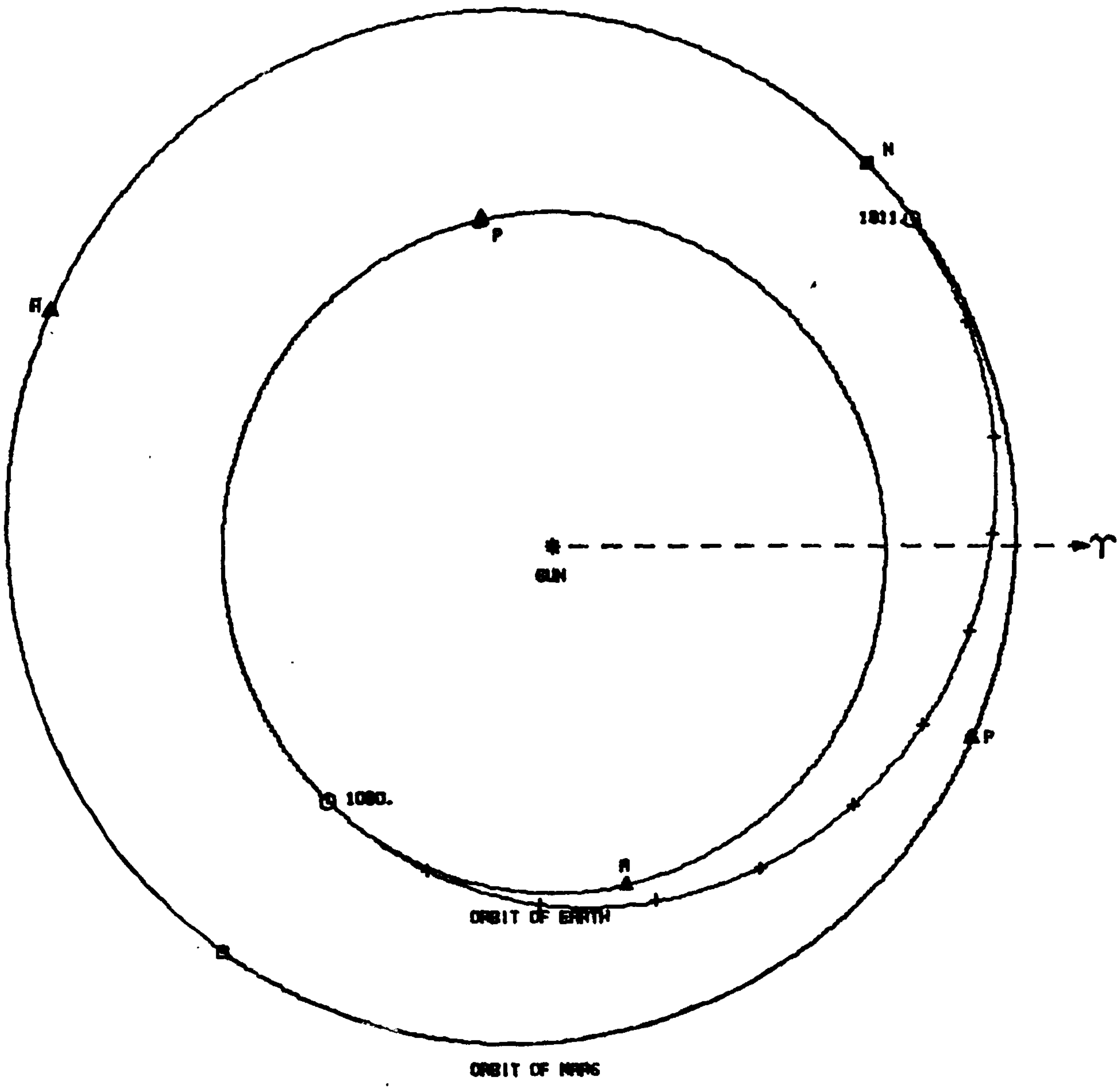

Solar Electric Propelled Mars Orbiter 1971

Launch on May 8, 1971
Flight Time 231 days

FIGURE 1

PRELIMINARY

1 November 1966

TABLE 2

Solar Electric Propelled Mars Orbiter 1973

	Calendar Date	Julian Date
Leave Earth sphere of influence, T_o ($t = 0$ hrs)	Jul 18, 1973	2441881.9180
Vis-Viva Energy, $C_3 = 4.284250\ km^2\ s^{-2}$		
Arrive near Mars, T_f ($t = 290$ days + 6 hrs)	May 4, 1974	2442172.168
Transfer Angle = 193.647^o		

	T_o		T_f			
	Earth Ephemeris	Hughes	Mars Ephemeris	Hughes	Mod. ITEM	Δ(MI-H)
X,AU	-.43433157	.43990889	-1.0192191	-1.0210939	-1.0198274	+.0020112
Y,AU	-.91875923	-.91634484	1.2932204	1.29279030	1.2975192	+.0047289
Z,AU	.000043574721	.00082652	.05217836	-.04178525	.04995[illegible]	+.0917366
$\dot{X}$,EMOS	.88761689	.97181858	-.60714355	-	-.57883632	-
$\dot{Y}$,EMOS	.42359476	.46364744	-.43483581	-	-.40812102	-
$\dot{Z}$,EMOS	-.000047628808	-.01350321	.00561932	.00640918	.01433338	+.00792421
S/C Mass, kgm	2267.6			-	2060.6	-
Ratio S/C Mass @ T_f/T_o				-	.9087	-
Approach Speed to Mars, $km\ s^{-1}$				1.151	1.188	+.037

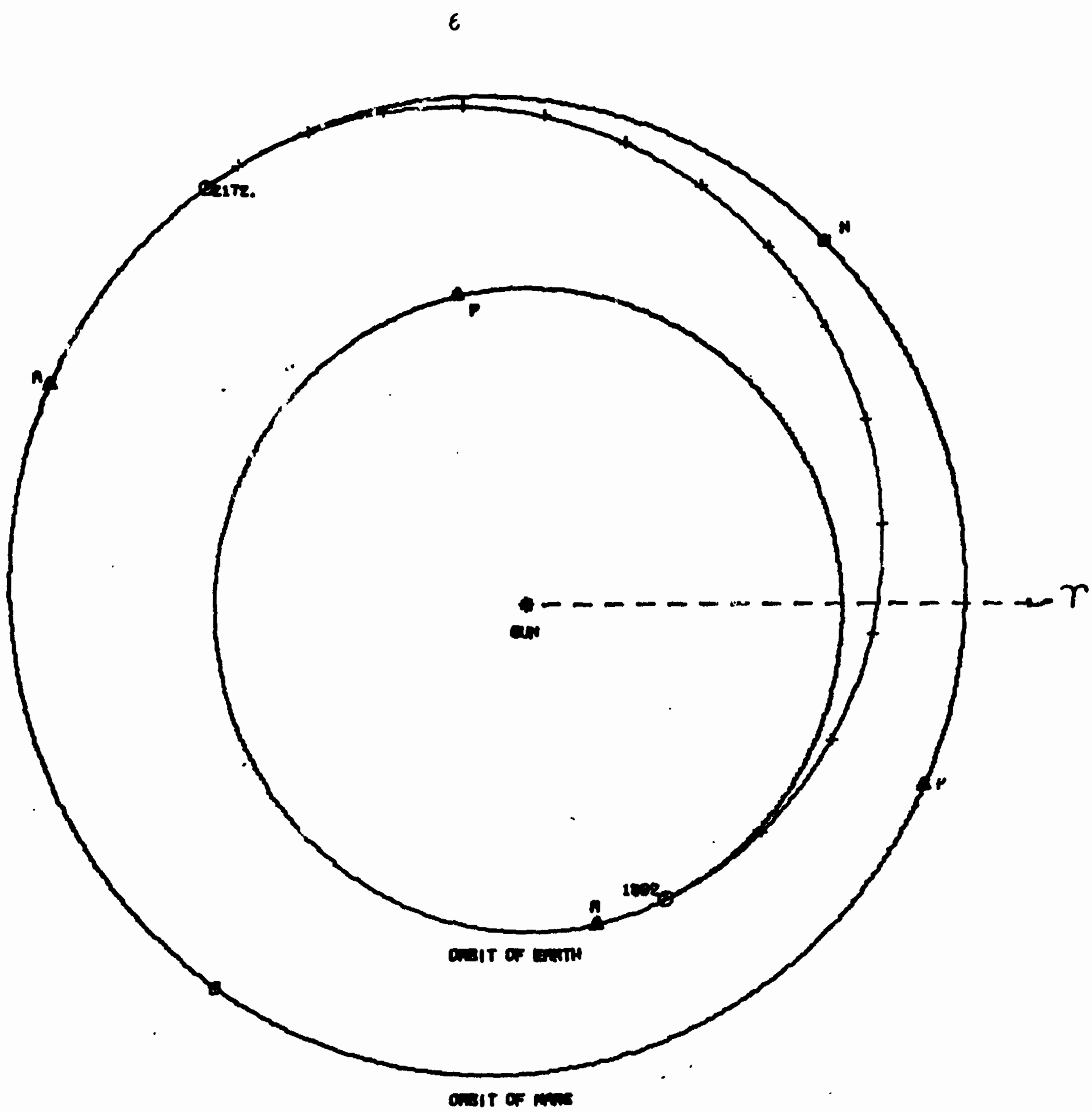

Solar Electric Propelled Mars Orbiter 1973

Launch on July 18, 1973
Flight Time 290 days

FIGURE 2

TABLE 3

Solar Electric Propelled Mars Orbiter 1975

	Calendar Date	Julian Date
Leave Earth sphere of influence, t_o ($t = 0$ hrs)	Aug 17, 1975	2442641.7036
Vis-Viva Energy, $C_3 = 5.597589\ km^2\ s^{-2}$		
Arrive near Mars, T_f ($t = 400$ days + 10.5 hrs)	Sep 20, 1976	2443042.141
Transfer Angle = 246.298^o		

	T_o		T_f			
	Earth Ephemeris	Hughes	Mars Ephemeris	Hughes	Mod. ITEM	Δ(MI-H)
X,AU	.81207179	.81588832	-1.3840137	-1.3835629	-1.4089081	-.0253452
Y,AU	-.60467791	-.59990672	-.79574684	-.79677297	-.78002986	+.0167431
Z,AU	.000027215108	.0025008	.01693795	-.21129974	.02414513	+.2354449
$\dot{X}$,EMOS	.58055977	.63155264	.43701443	-	.41091670	-
$\dot{Y}$,EMOS	.79860931	.86652473	-.63626897	-	-.62467903	-
$\dot{Z}$,EMOS	-.000080109686	-.00291483	-.02409940	.02103958	.00112034	-.0199092
S/C Mass, kgm		2395.2		-	2130.7	-
Ratio S/C Mass @T_f/T_o				-	.8896	-
Approach Speed to Mars, $km\ s^{-1}$				.908	1.135	-.227

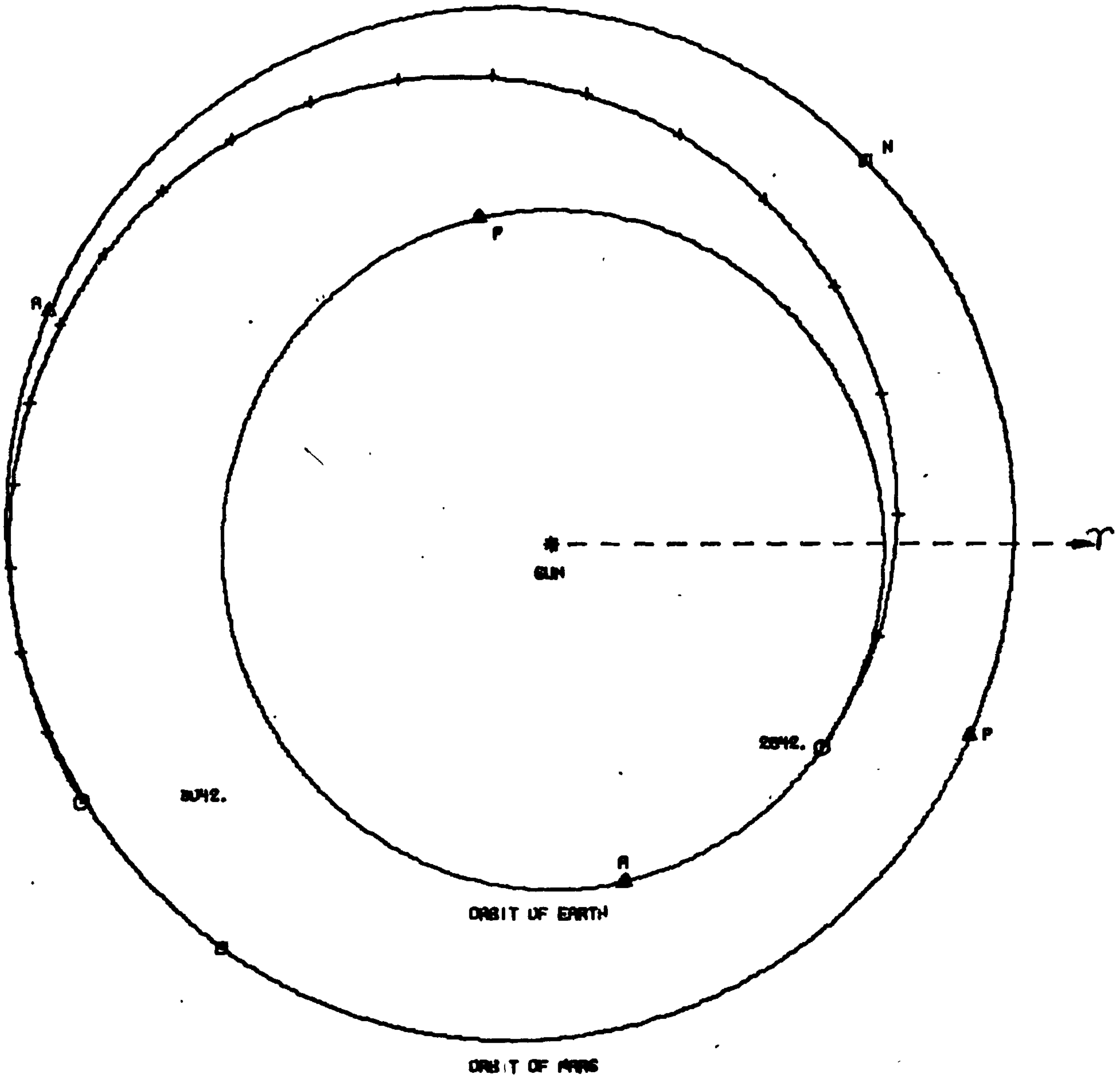

Solar Electric Propelled Mars Orbiter 1975

Launch on Aug 17, 1975
Flight Time 400 days

FIGURE 3

Solar Electric Propelled Mars Orbiter 1977

	Calendar Date	Julian Date
Leave Earth sphere of influence, t_o (t = 0 hrs)	Sep 6, 1977	2443393.2549
Vis-Viva Energy, $C_3 = 4.062134\ km^2 s^{-2}$		
Arrive near Mars, T_f (t = 430 days + 6 hrs)	Nov 11, 1978	2443823.505
Transfer Angle = 273.597^o		

	T_o		T_f			
	Earth Ephemeris	Hughes	Mars Ephemeris	Hughes	Mod. ITEM	Δ(MI-H)
X,AU	.96696105	.96886610	-.30366671	-.30282720	-.32020429	-.0173771
Y,AU	-.28384636	-.27811922	-1.4476876	-1.4480352	-1.4541280	-.0060928
Z,AU	.000015571713	.00126240	-.02318347	-.1403094	-.02338891	+.1169205
$\dot{X}$,EMOS	.26574941	.28592724	.82800118	-	.79959284	-
$\dot{Y}$,EMOS	.95609573	1.0262130	-.09755981	-	-.10393839	-
$\dot{Z}$,EMOS	-.000051816124	.01510697	-.02224486	.02654276	.00504140	-.02150136
S/C Mass, kgm	2534.5			-	2238.1	-
Ratio S/C Mass @ T_f/T_o				-	.8831	-
Approach Speed to Mars, km s^{-1}				1.108	1.188	+.080

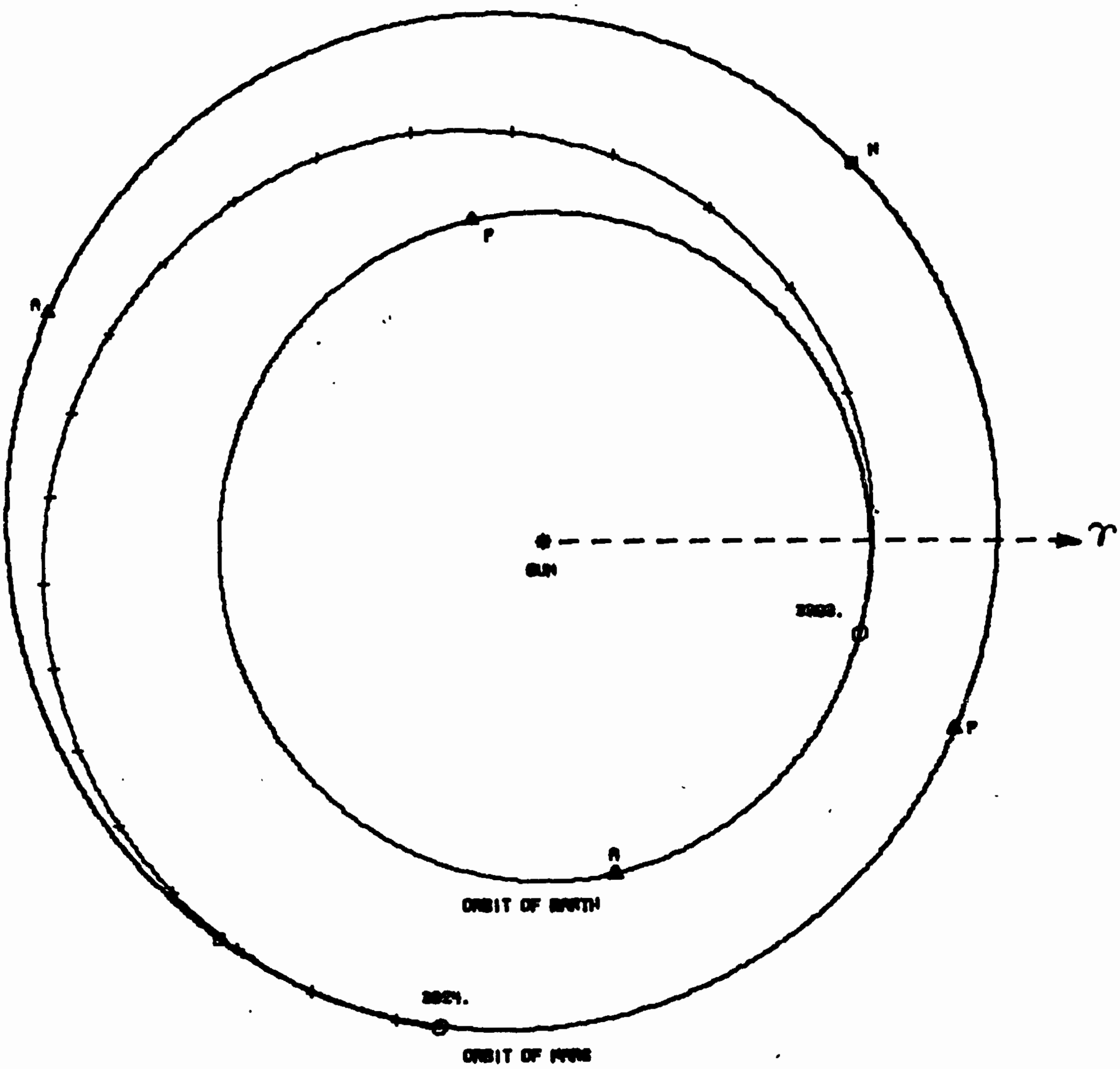

Solar Electric Propelled Mars Orbiter 1977

Launch on Sep 6, 1977
Flight Time 431 days

FIGURE 4

PRELIMINARY

1 November 1966

TABLE 5

Solar Electric Propelled Mars Orbiter 1979

	Calendar Date	Julian Date
Leave Earth sphere of influence, t_o (t = 0 hrs)	Oct 1, 1979	2444148.4097
Vis-Viva Energy, C_3 = 3.094429 $km^2\ s^{-2}$		
Arrive near Mars, T_f (t = 405 days + 9 hrs)	Nov 10, 1980	2444553.785
Transfer Angle = 274.412°		

	T_o		T_f			
	Earth Ephemeris	Hughes	Mars Ephemeris	Hughes	Mod. ITEM	Δ(MI-H)
X,AU	.99196021	.99148069	.32090550	.32210213	.30967932	-.0124228
Y,AU	.13429613	.13982004	-1.3917614	-1.3919647	-1.4034039	-.0114392
Z,AU	-.000015809666	.00254740	-.03723094	-.08671704	-.03642319	+.0502938
$\dot{X}$,EMOS	.15078670	.1585372	.82438581	-	.78569897	-
$\dot{Y}$,EMOS	.98724151	1.0475929	.25227699	-	.23144750	-
$\dot{Z}$,EMOS	-.000028900089	.02770106	-.01476223	.02134158	.00754481	-.0137968
S/C Mass, kgm	2622,3			-	3232.4	-
Ratio S/C Mass@ T_f/T_o				-	.8860	-
Approach Speed to Mars, km s^{-1}				1.385	1.467	+.082

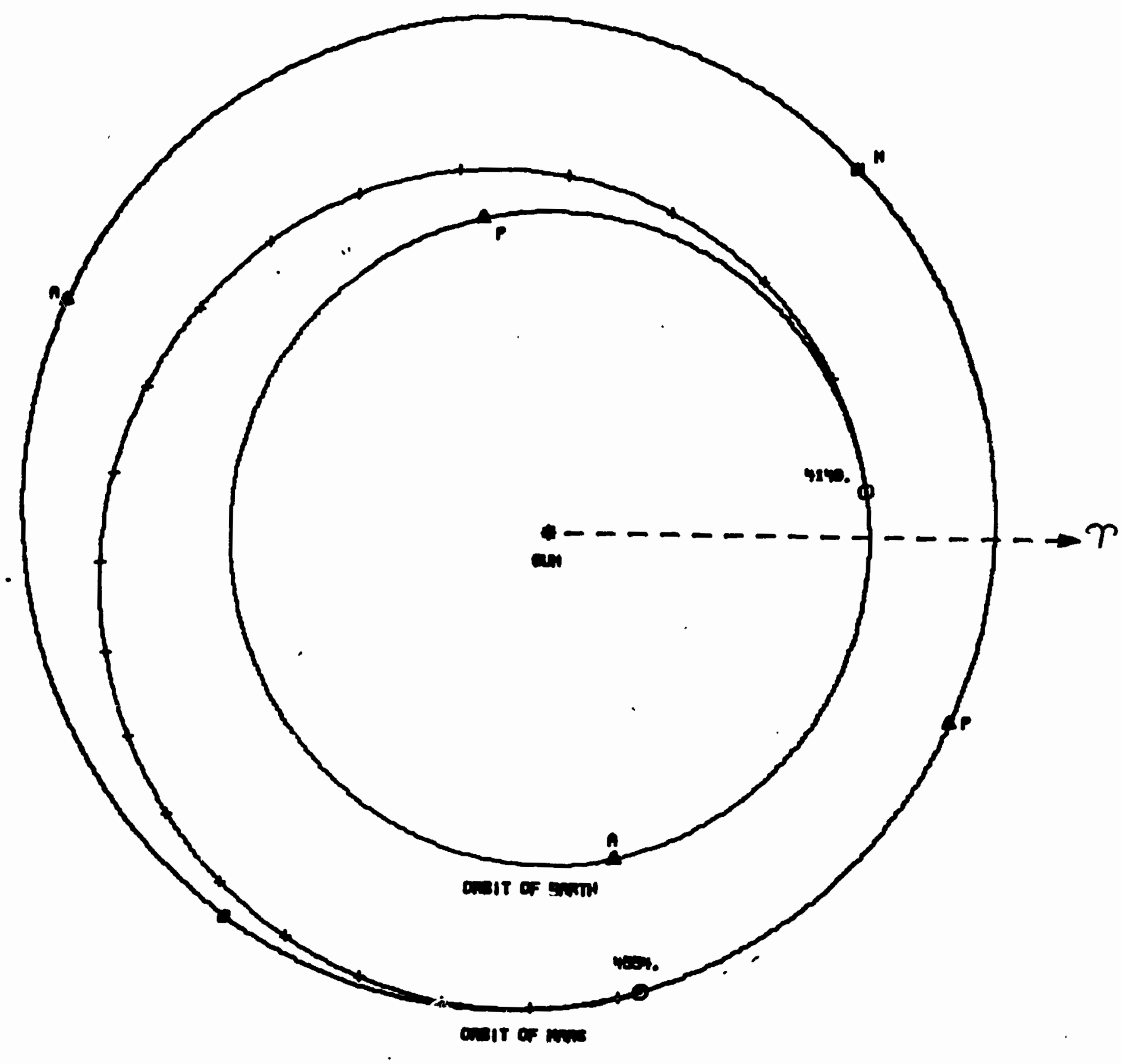

Solar Electric Propelled Mars Orbiter 1979

Launch on Oct 1, 1979
Flight Time 406 days

FIGURE 5

(1) Changes to increase flexibility

(a) The program has been converted into a subroutine capable of integrating a trajectory segment, so that a trajectory of any configuration can be created by making multiple calls on the integration routine.

(b) The number of planets has been increased from four to nine.

(c) The ability to stop the trajectory precisely on a given time, flight path angle, or radius magnitude has been included. This allows more freedom in the selection of parameters for iteration and optimization.

(d) In addition to programmed thrust modes, the ability to integrate the adjoint equations has been included.

(2) Changes to increase efficiency

(a) Time has been replaced by beta as the independent variable of the integration. Beta is defined by the following equation:

$$-\beta^2/a = \theta^2$$

where a is the semi-major axis of the orbit and θ is the incremental eccentric anomaly. This change allows Kepler's equation solution to be obtained without iteration, and it allows a more favorable step size to be chosen for the numerical integration.

(b) The ephemeris routine was modified to place all necessary ephemeris data in core at the same time. This eliminates tape manipulation during the computation of a trajectory but restricts the program to computers of at least 65K words of core storage.

(c) The integrator has been changed from single step to multi-line integration. A table of 25 points is used. The value of this is:

(i) The number of Runge-Kutta steps necessary for starting is reduced. This allows starting of the sixth order integration in about one-third of the time previously required.

(ii) Updating of the table is more efficient since it is only required once every 18 steps instead of every step.

(iii) Plenty of points are available for interpolation if values are desired which are not contained exactly in the table.

(iv) Editing of the tables is more efficient.

(d) Three modes of integration (all sixth order) have been included. These are:

(i) Backwards difference predictor only.

(ii) Backwards difference predictor with a central difference corrector.

(iii) Iterative central difference corrector.

Two modes of starting are included:

(i) 4 to 1 Runge-Kutta and backward difference predictor.

(ii) Iterative central difference corrector.

These modes allow any necessary integration accuracy with a corresponding amount of computer time.

III. JUPITER FLYBY STUDY

A. Introduction

Advances in hardware technology of solar powered, electric rocket propelled space vehicles have, in recent years, been sufficient to justify examination of the possible usefulness of this type of propulsion in two ways: (1) performance of higher energy missions without requiring uprated launch vehicles, and (2) early testing of advanced electric rocket thruster technology without the radiation problems inherent in nuclear powered systems. The first way requires that solar electric propelled vehicles compare favorably to existing systems for sufficiently important classes of missions. Indeed, if this were strongly the case, then solar power could become a key step on the road to future advanced propulsion systems. Recognizing the possibilities for solar-powered vehicles, the Jet Propulsion Laboratory (JPL) in 1966 incorporated studies of solar-powered vehicles in their advanced programs. An examination was conducted of the possible missions into which solar-power might fit, and from the resulting possibilities, the Jupiter flyby was chosen for an in-depth study. This mission was chosen because it represents the first advanced mission which might benefit to a major extent from solar-electric propulsion. This research was undertaken to support the JPL effort by analytical and programming work including clarification of the optimum mode by carrying out the preliminary mission analyses reported herein.

B. Optimum Solar Electric Propelled Jupiter Flyby Trajectories

A study of optimum flyby trajectories to Jupiter using solar electric propulsion for flight times from 600 to 900 days is reported in this section. The launch vehicle used was the Atlas SLV3C/Centaur. A "flyby" trajectory matches the position of the target planet - in this case Jupiter - with no constraint on the velocity. Optimum in this report means maximized payload or net spacecraft mass at the target.

Low-thrust optimization of the Jupiter flybys was accomplished by the Gordon 2 computer program which was developed at Princeton under Contract NASr-231. This program is a two-body, two-dimensional, finite thrust, trajectory optimization program. In addition to optimizing the thrust direction and the switch times of the propulsion system, other significant parameters associated with the trajectory can be optimized such as jet velocity, power level, hyperbolic excess velocity, launch-time and flight time.

Modifications to the program for this study include

(1) The capability of power variation as a function of solar radius, including the appropriate adjoint equations.

(2) Subroutines which give the launch vehicle performance for a variety of launch vehicles, and solar array and electric rocket ion engine performance.

(3) Addition of an ephemeris routine which computes initial and final conditions used in the iteration, given the Julian launch date and trip time. A second routine searches the ephemeris tape for launch configurations which correspond to given boundary conditions. This permits the identification of appropriate launch dates which correspond to optimum angle trajectories.

(4) Addition of sweep capabilities for several parameters including launch date, trip time, jet velocity, power, and hyperbolic excess velocity.

(5) Provision for a finite hyperbolic velocity at the arrival planet. The magnitude of the hyperbolic velocity can be specified and its direction specified or optimized.

(6) Improved integration and iteration procedures. The integration was improved from second order to fourth order in the predictor-corrector scheme. The iteration routines were improved for greater stability through the inclusion of an automatic correction limiter. The results are a faster and more uniform convergence.

The following assumptions were used in the Jupiter flyby trajectory optimization:

(1) The space vehicle is considered to be comprised of power supply and thrusters, propellant, propellant tankage and payload. The payload includes all items not included in the other categories. Mass of the power system is assumed to be proportional to total power. The power system specific mass, α, is taken to be 30 kg kWe^{-1} throughout the study (except for the sensitivity analyses). Tankage mass is assumed to be proportional to fuel expended, with the factor of proportionality 0.05. No specific allowance is made for structure mass, so it must be considered part of the payload.

(2) Jupiter and Earth were assumed to be in coplanar, circular orbits. Departure and arrival coordinates were taken to be the planetary centers and their mass was ignored during the low thrust heliocentric trajectory. Departure and arrival dates were taken to give an optimum central angle.

(3) The launch vehicle was the Atlas SLV3C/Centaur. The relationship between injected mass and hyperbolic excess velocity was obtained from the NASA OSSA Launch Vehicle Estimating Factors[2] and is shown in Figure 6 as a curve fit and its derivatives.

(4) Except for sensitivity analyses all trajectories optimized power level, jet velocity, and hyperbolic excess velocity.

LAUNCH VEHICLE PERFORMANCE

Launch Capability of the Atlas (SLV3C)/Centaur for the period 1973—1977

Ref: N A S A, Launch Vehicle Estimating Factors for Generating OSSA Prospectus 1967, November 1966

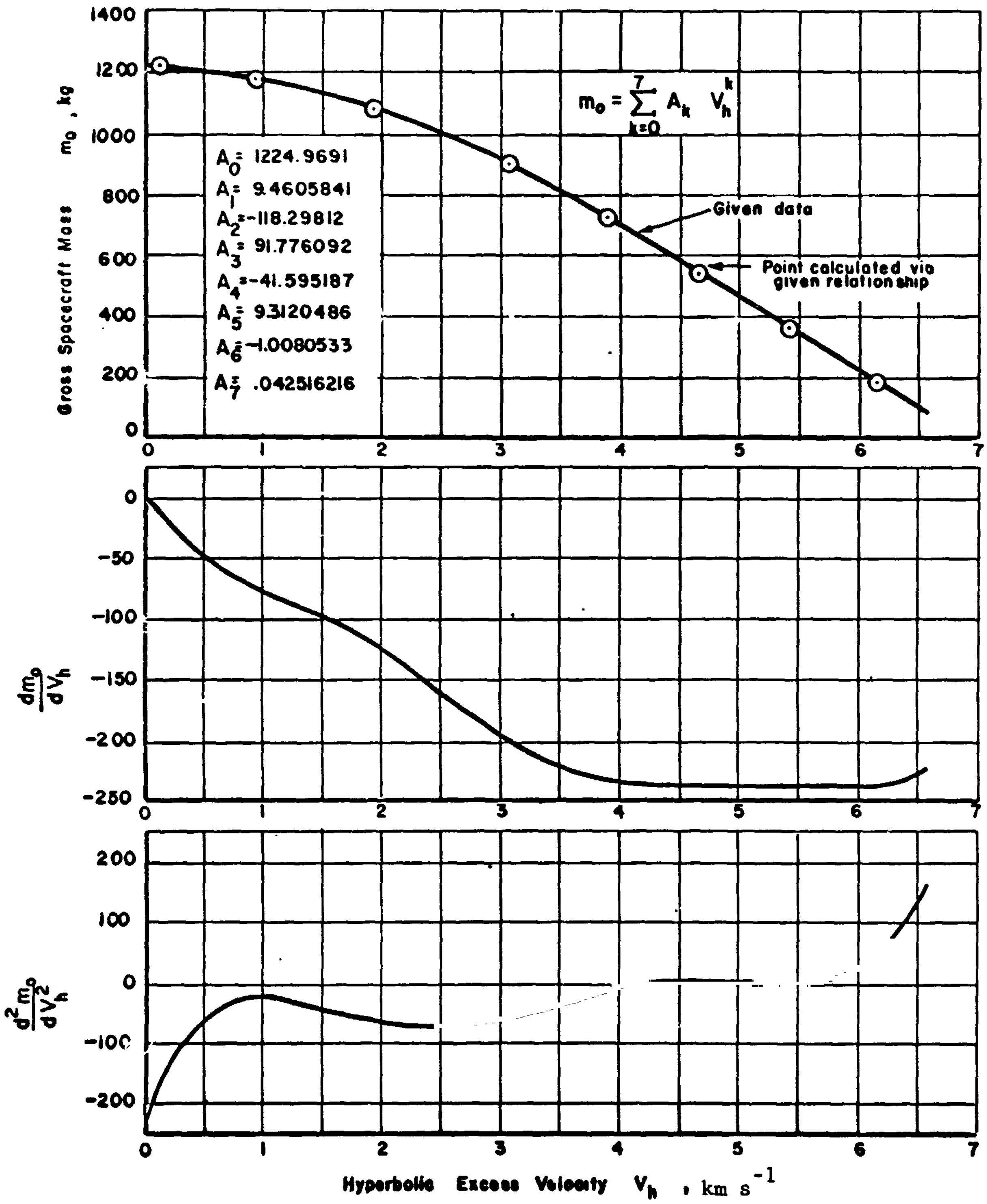

Curve Fit of Gross Spacecraft Mass Versus Hyperbolic Excess Velocity

FIGURE 6

(5) Propulsion system efficiency is assumed to be a function of jet velocity. This relationship, was provided by NASA Headquarters[3] and is shown in Figure 7.

(6) The variation of solar power with distance from the sun was obtained from the Hughes Study Report[1]. The relationship is shown in Figure 8.

(7) The range of flight times investigated was 500 to 900 days.

One of the interesting results of the study was the identification of three different modes for solar electric propelled Jupiter flybys over the range of flight times investigated. Mode 1, shown in Figure 9, is a direct flight with thrust always acting in the general direction of the velocity and energy always increasing. Travel angles for this mode are typically four radians. Mode 2, shown in Figure 10, requires an initial retro-thrust thus decreasing energy and allowing the spacecraft to fall in toward the Sun. At the perihelion of this trajectory, where power is maximum, the thrust direction has swung around and now supports the motion so the spacecraft energy increases. Travel angles for this mode are typically six radians. Mode 3, shown in Figure 11, has three different phases where the thrust alternately supports, opposes and again supports the motion and the energy is correspondingly increased, decreased, and increased. These trajectories are typically eight radians.

The principal result, a plot of payload vs travel time is shown in Figure 12. For short travel times, Mode 1 is the best; whereas, for longer trip times Mode 3 is best. For the particular vehicle characteristics used, the crossover point is about 870 days. Mode 2 is never optimum (except locally). Figures 13, 14 and 15 show further details on Modes 1, 2 and 3, respectively: power, hyperbolic excess velocity and jet velocity are plotted versus trip time.

ELECTROSTATIC (ION) ELECTRIC ROCKET PERFORMANCE

Electron Bombardment Thruster with Cesium for the Period 1973–1977

Ref: N A S A (J P. Mullin) Letter Dated January 19, 1967

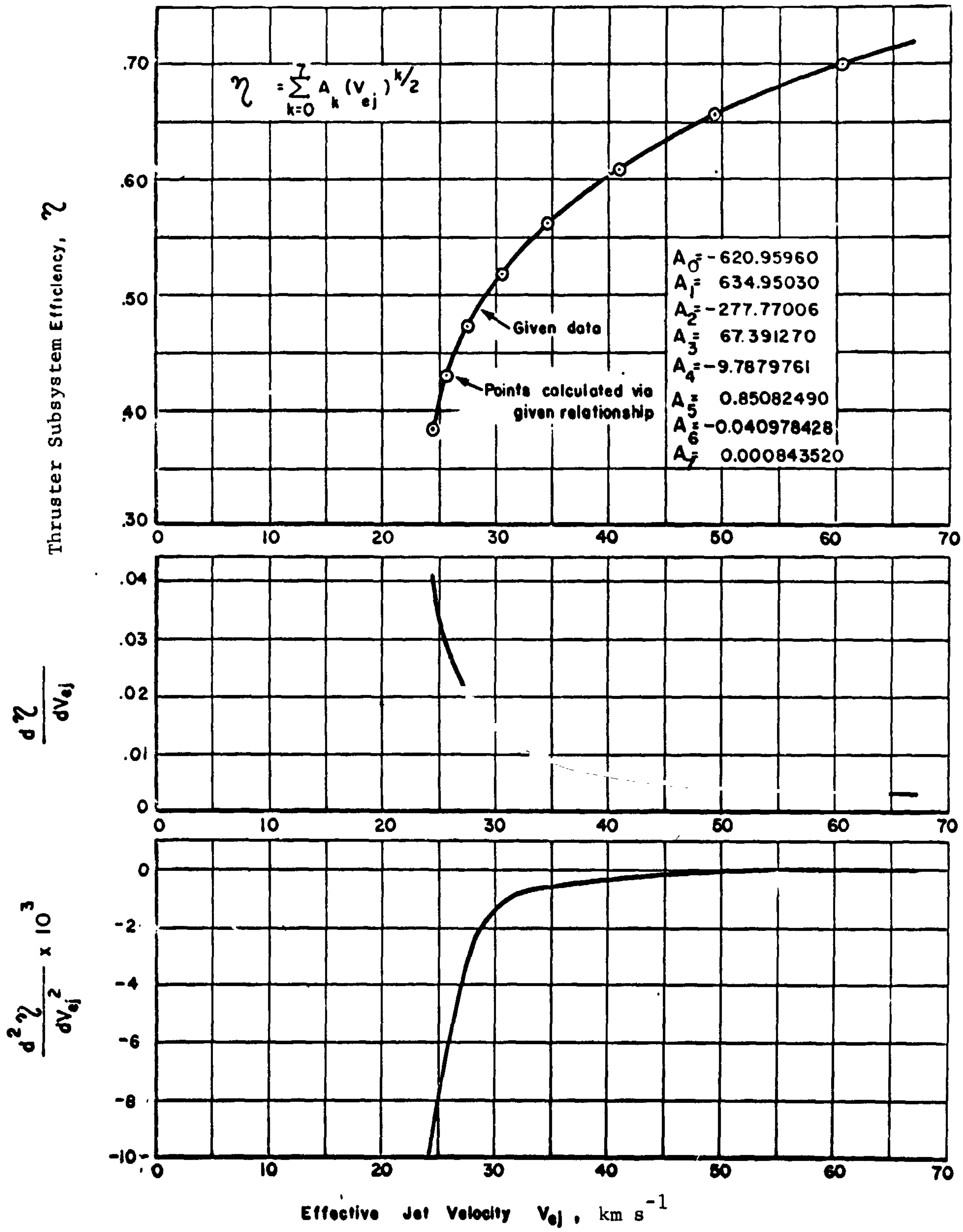

Curve Fit, Including First and Second Derivatives, of Overall Effiency vs. Effective Jet Velocity

FIGURE 7

SOLAR ELECTRIC ARRAY PERFORMANCE

Solar Electric Array Technology for the Period 1973 — 1977

Ref: Table A-3 Hughes Report SSD 60374R, December 1966.(1)

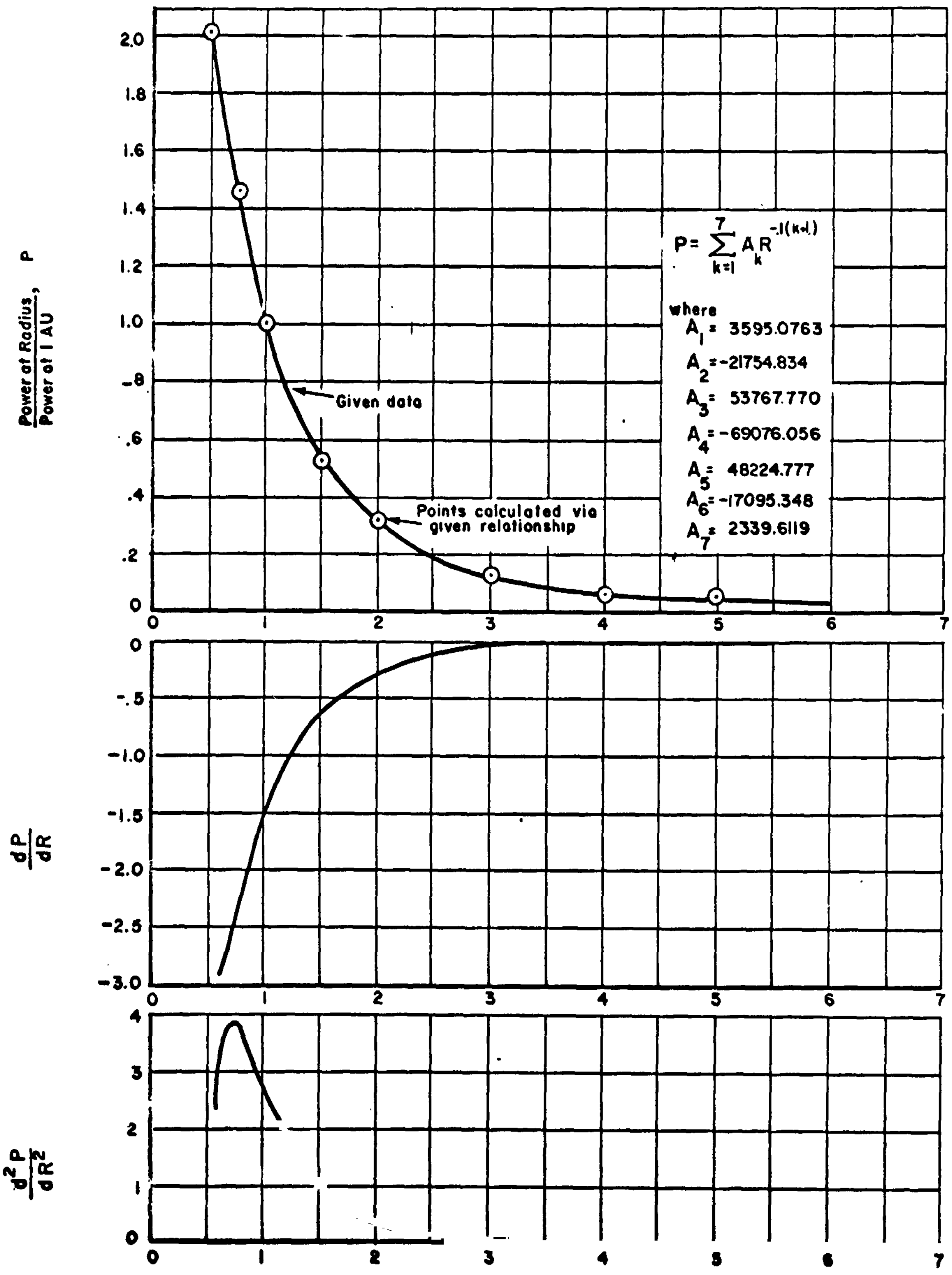

Curve Fit of Power Versus Radius

FIGURE 8

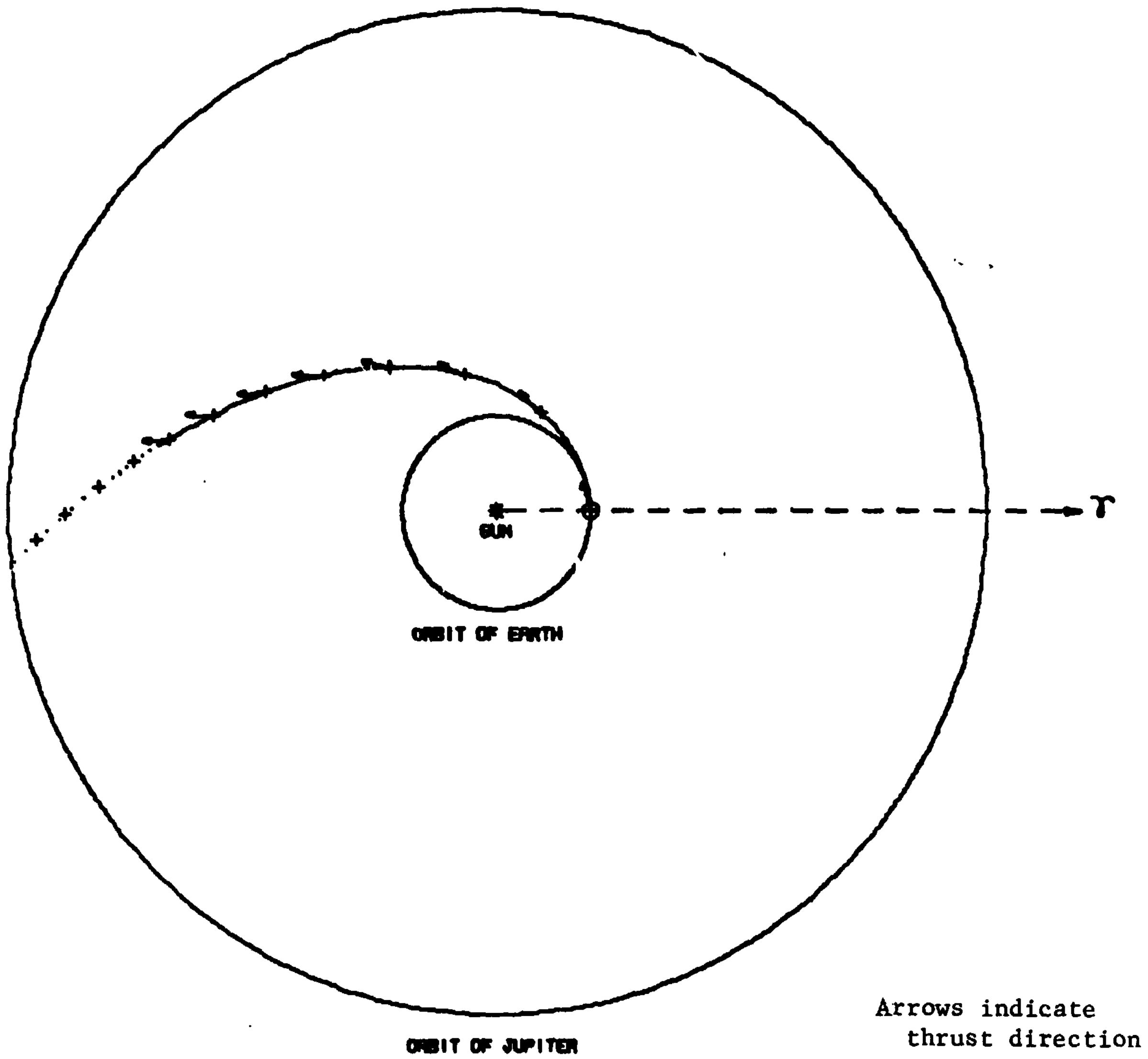

Jupiter Flyby Trajectory - Mode 1

Flight Time 600 days
Travel Angle 3.25 rad.

FIGURE 9

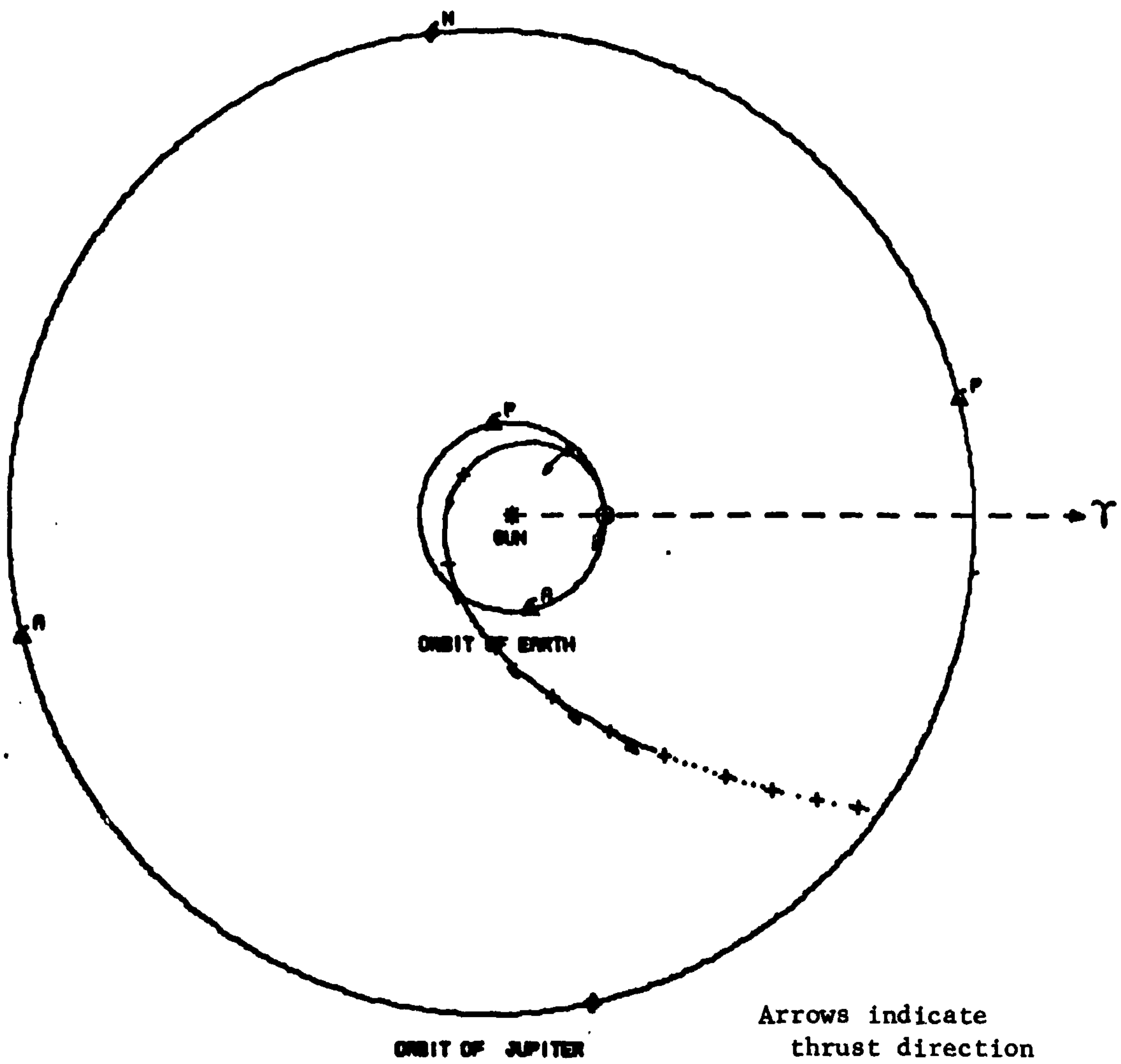

Jupiter Flyby Trajectory - Mode 2

Flight Time 600 days
Travel Angle 5.65 rad.

FIGURE 10

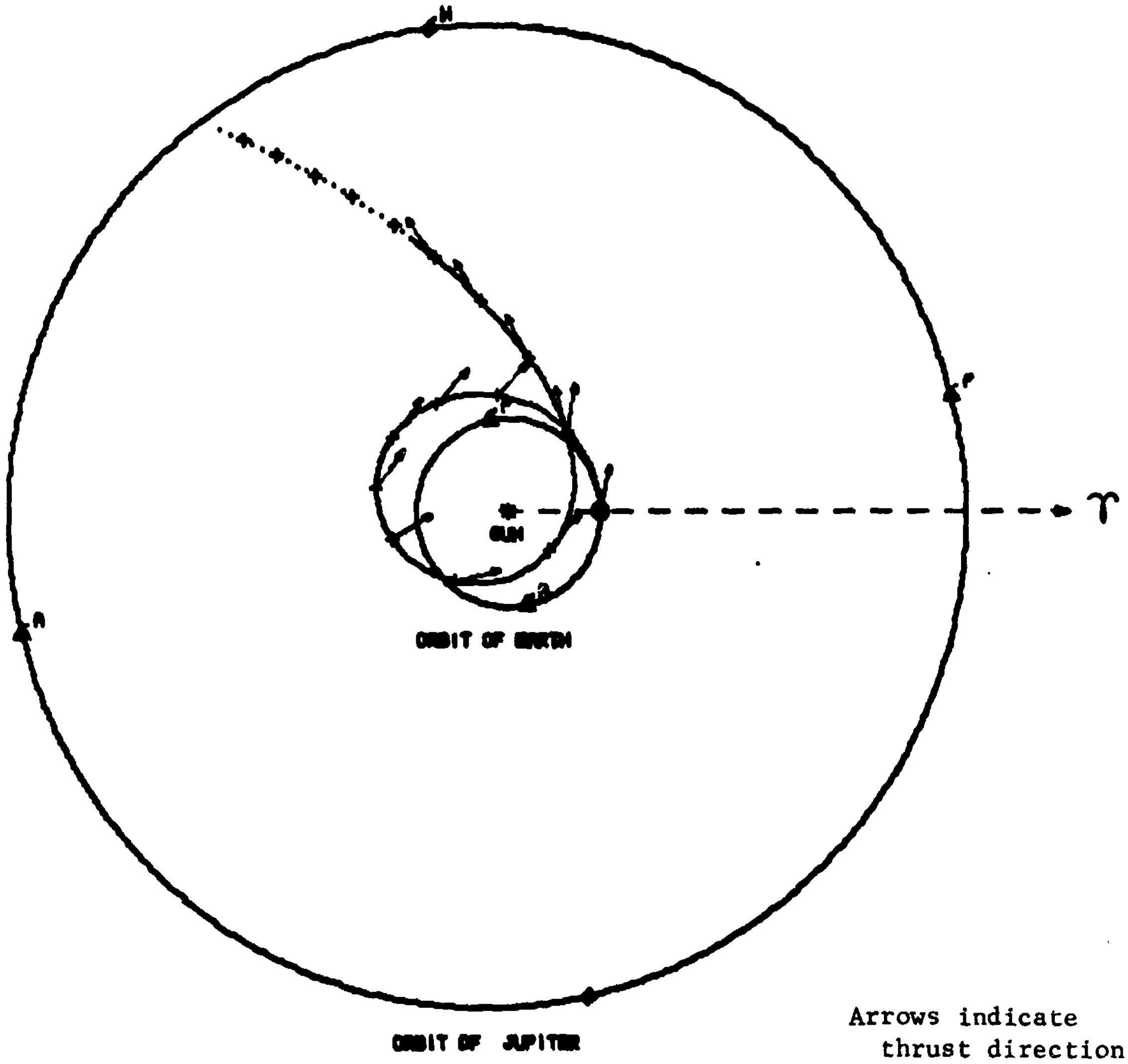

Jupiter Flyby Trajectory - Mode 3

Flight Time 900 days
Travel Angle 8.525 rad.

FIGURE 11

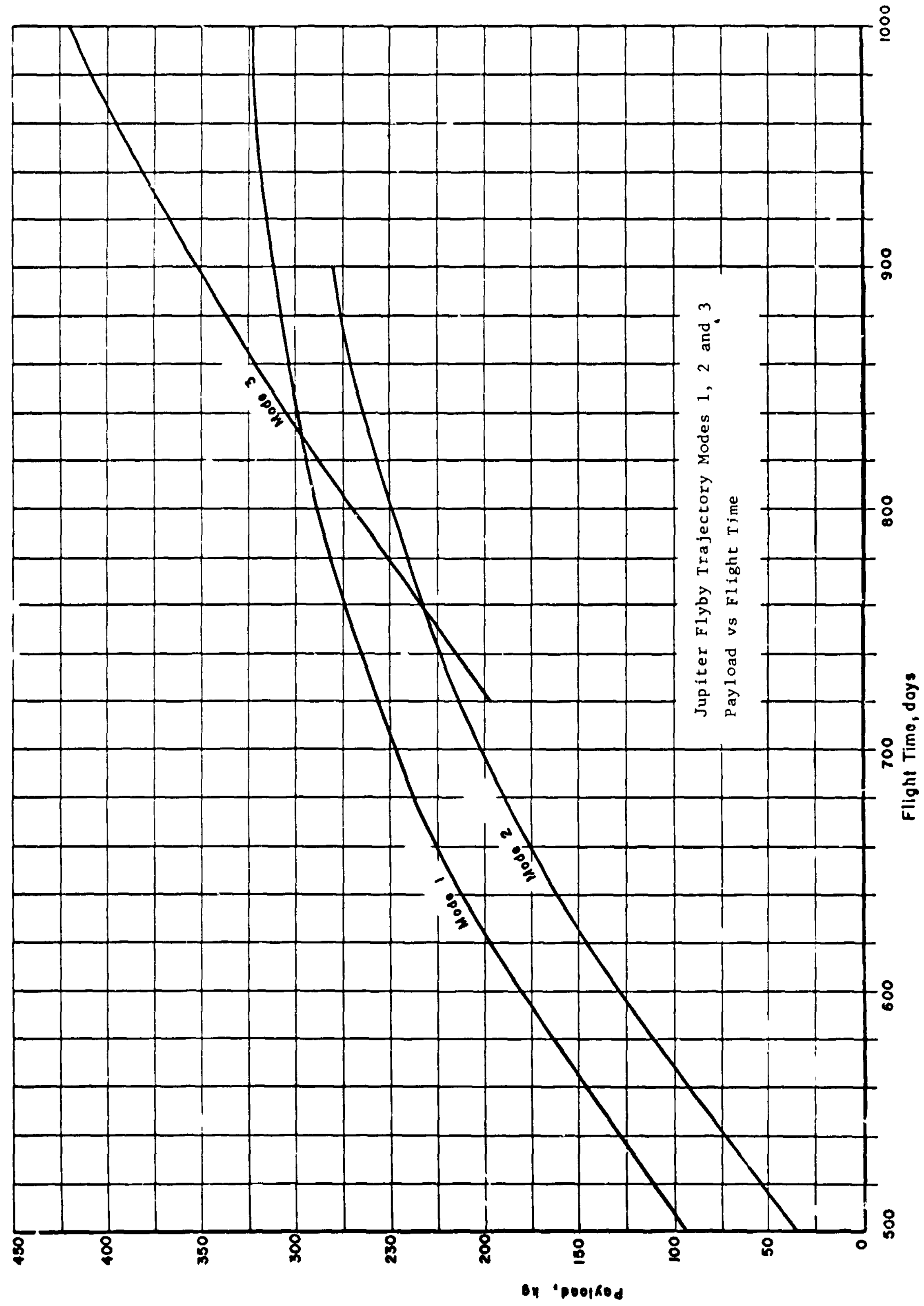
Jupiter Flyby Trajectory Modes 1, 2 and 3
Payload vs Flight Time
Mode 1
Mode 2
Mode 3
Payload, kg
450
400
350
300
250
200
150
100
50
0
Flight Time, days
500
600
700
800
900
1000

FIGURE 12

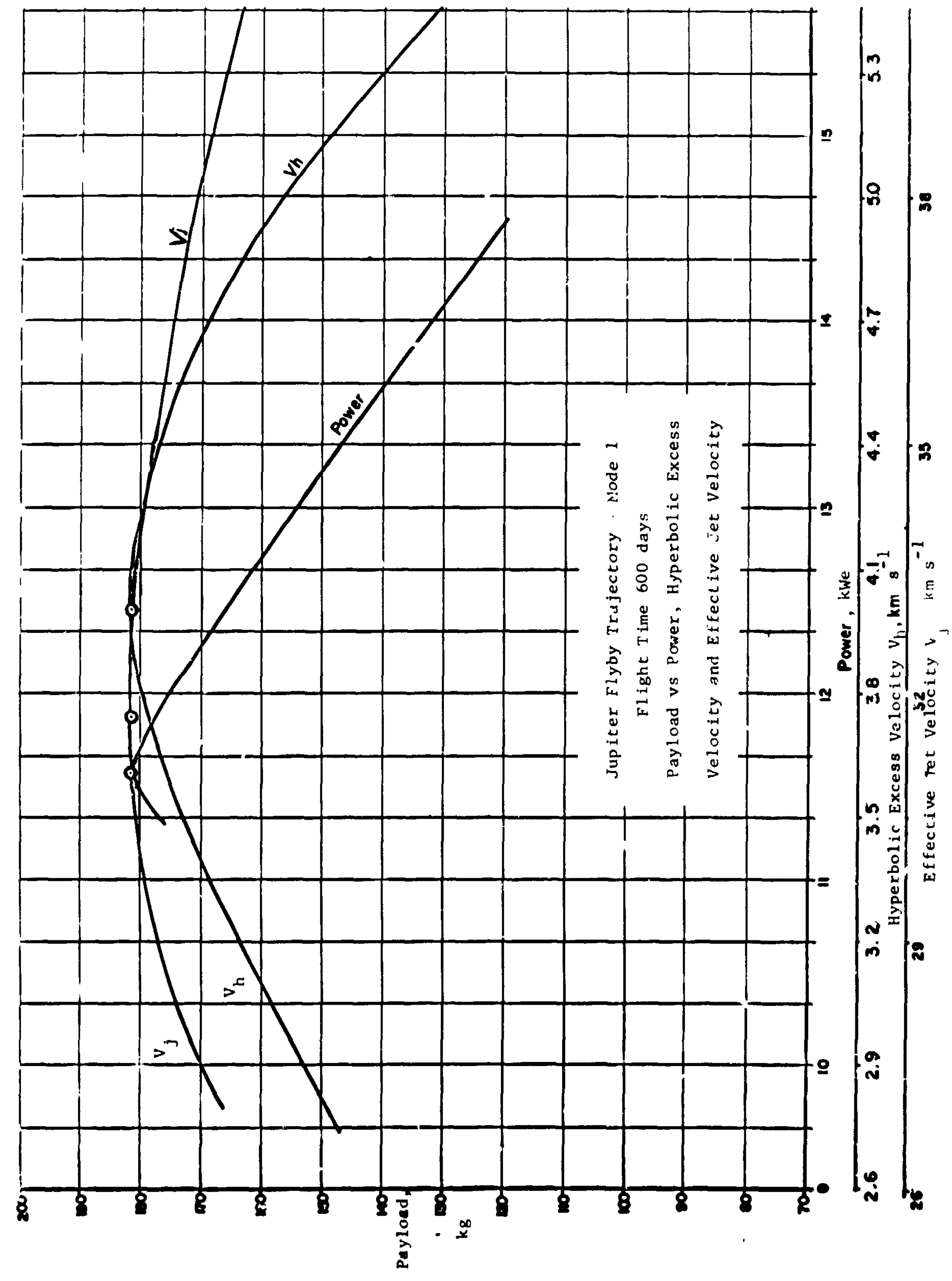

Jupiter Flyby Trajectory - Mode 1
Flight Time 600 days
Payload vs Power, Hyperbolic Excess
Velocity and Effective Jet Velocity
Payload, kg
Power, kWe
Hyperbolic Excess Velocity V_h, km s^{-1}
Effective Jet Velocity V_j km s^{-1}
Power
V_h
V_j

FIGURE 13

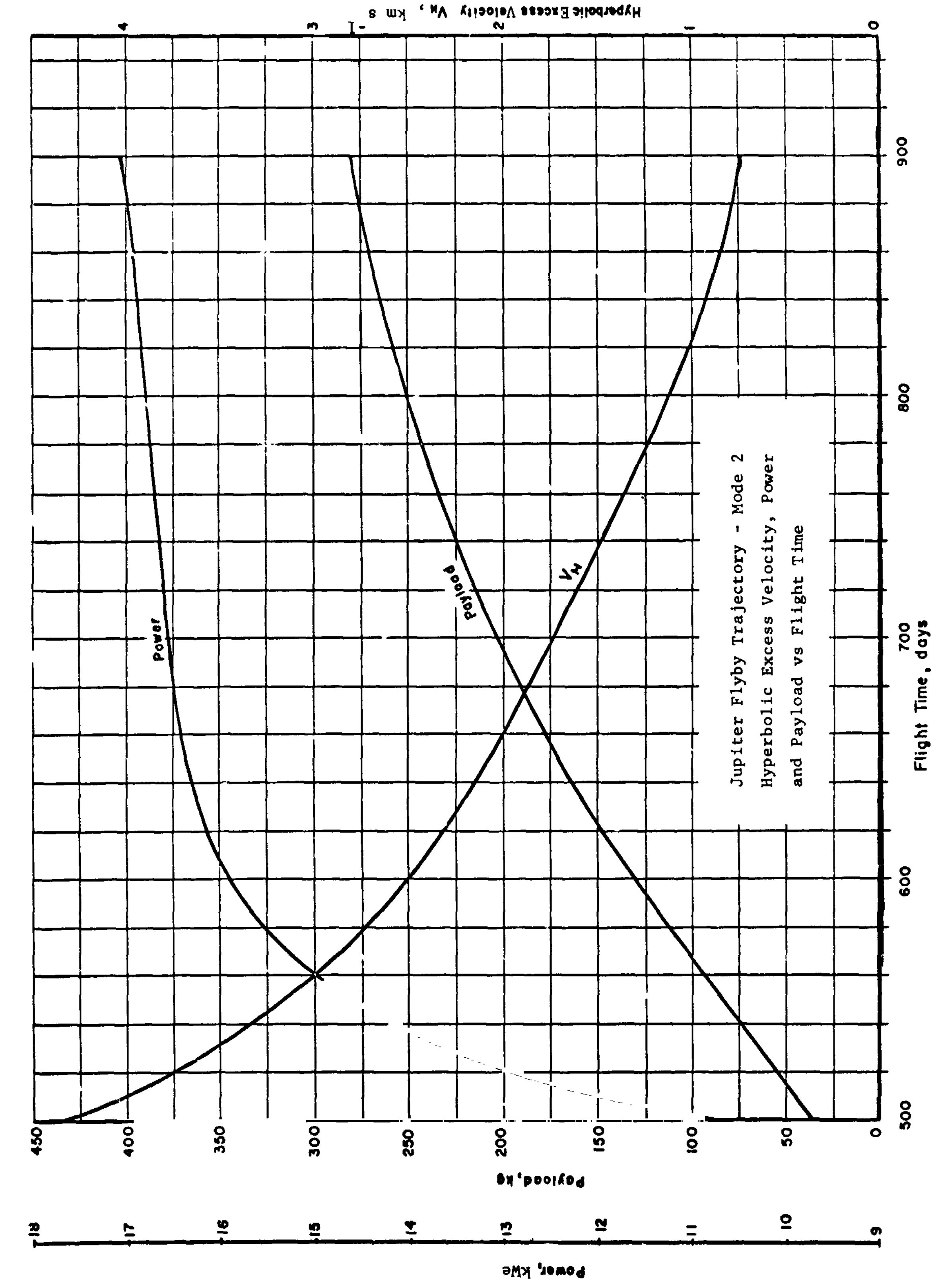
Jupiter Flyby Trajectory - Mode 2
Hyperbolic Excess Velocity, Power
and Payload vs Flight Time
Power
Payload
V_H
Flight Time, days
500
600
700
800
900
Payload, kg
0
50
100
150
200
250
300
350
400
450
Power, kWe
9
10
11
12
13
14
15
16
17
18
Hyperbolic Excess Velocity V_H, km s^{-1}
0
1
2
3
4

FIGURE 14

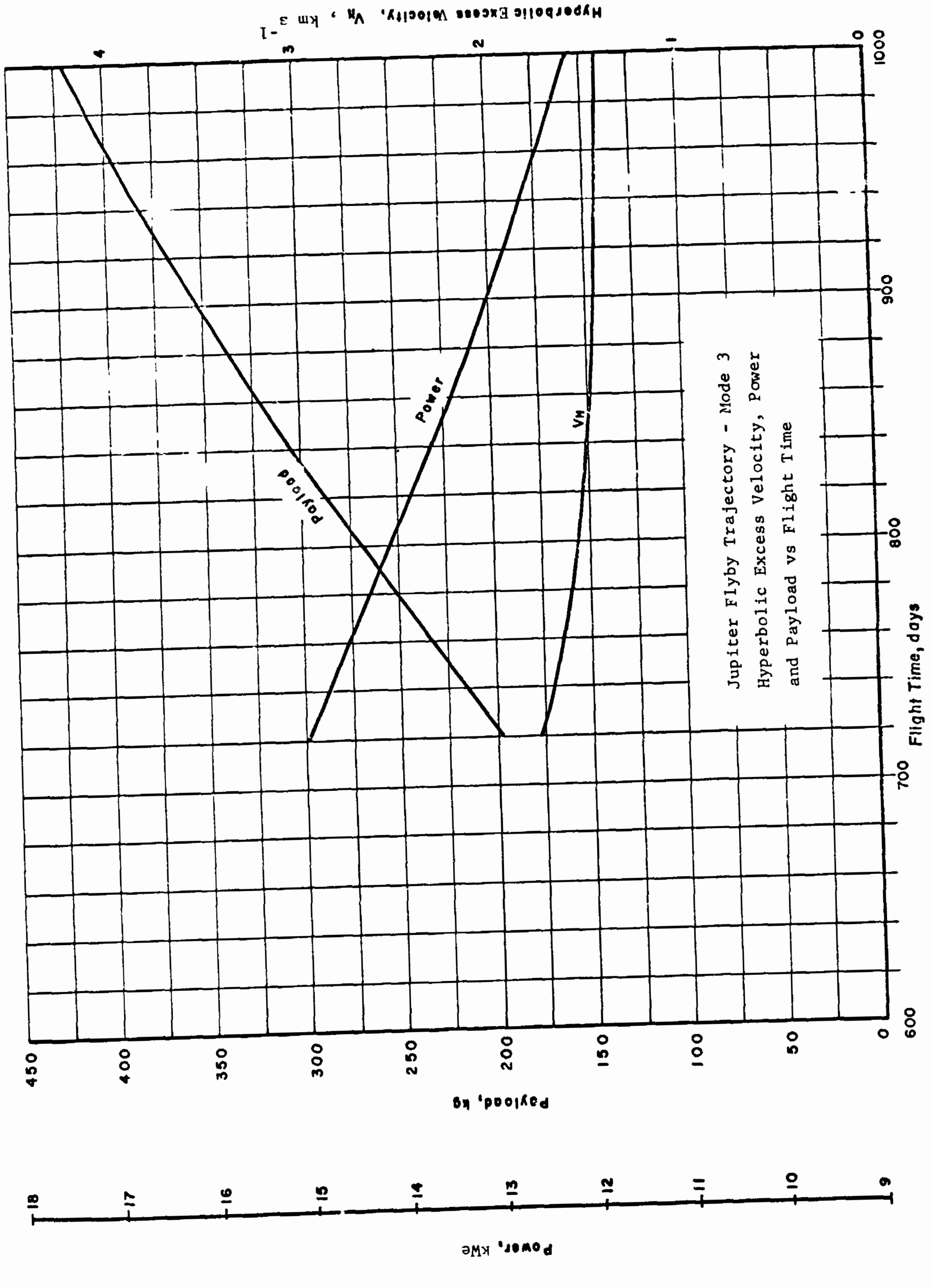
Jupiter Flyby Trajectory - Mode 3
Hyperbolic Excess Velocity, Power
and Payload vs Flight Time
Hyperbolic Excess Velocity, V_H, km s^{-1}
Payload, kg
Power, kWe
Flight Time, days
Payload
Power
V_H
600
700
800
900
1000
0
50
100
150
200
250
300
350
400
450
1
2
3
4
9
10
11
12
13
14
15
16
17
18

FIGURE 15

Figure 16 shows a typical (600 day) Mode 1 trajectory profile (See Figure 9); similarly, Figure 17 shows a profile for 900 day Mode 3 trajectory (See Figure 11).

The trajectories just described optimized power level, jet velocity, and hyperbolic excess velocity as well as the thrust program. The sensitivity of Mode 1 trajectories to off-optimum conditions and variation of prescribed parameters was also studied as described below.

Figure 18 shows the variation of payload versus hyperbolic excess velocity for a number of flight times. In this case the optimum is quite flat. Figure 19 shows the effect on payload of an improvement in powerplant specific mass over a range of flight times. The original trajectories were computed using $\alpha = 30.0$ kg kWe^{-1}. The effect of a reduction to $\alpha = 27.0$ and 24.0 is shown. For this plot, trajectories were re-optimized using these new values of α . Over the range investigated the effect on net mass is for practical purposes, linear with α , and independent of flight time. Figure 20 shows the effect of an improvement in thruster system efficiency over a range of flight times. For this plot, the η vs V_j curve, originally provided by Reference 3 was increased by 10 and 20%. The trajectories were then re-optimized. Again the improvement appears to be relatively independent of flight time.

To determine the effect upon payload of variations in power level, jet velocity, and hyperbolic excess velocity, two example trajectories were chosen. The first is a Mode 1, 600 day flight with payload of about 181 kg. This direct trajectory is similar to that plotted in Figure 9, and the actual trajectory profile is shown in Figure 21. Sensitivity of payload to the above parameters is shown in Figure 22.

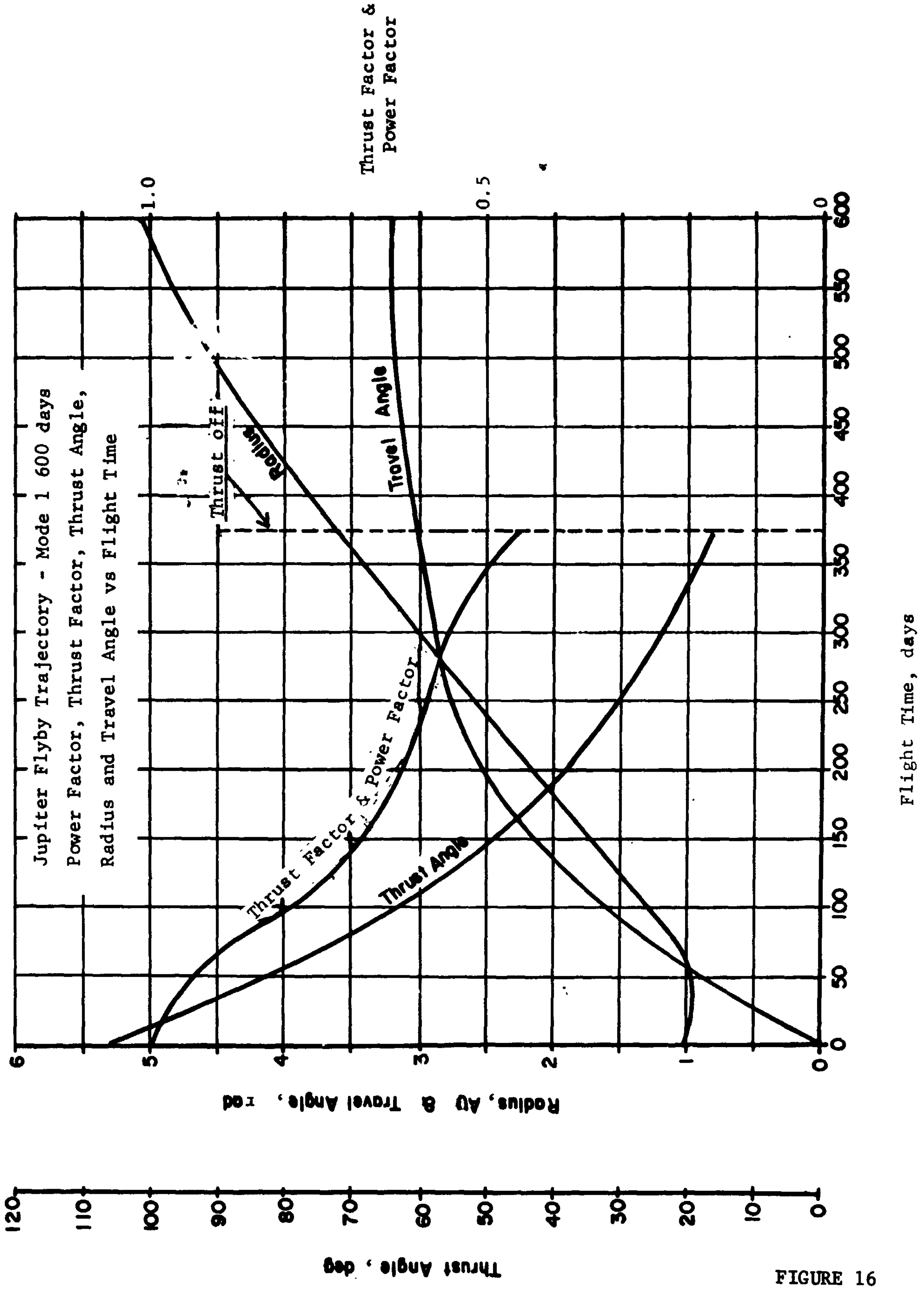

Jupiter Flyby Trajectory - Mode 1 600 days
Power Factor, Thrust Factor, Thrust Angle,
Radius and Travel Angle vs Flight Time
Thrust Factor &
Power Factor
1.0
0.5
0
Thrust off
Radius
Travel Angle
Thrust Factor & Power Factor
Thrust Angle
Flight Time, days
0
50
100
150
200
250
300
350
400
450
500
550
600
Radius, AU & Travel Angle, rad
6
5
4
3
2
1
0
Thrust Angle, deg
120
110
100
90
80
70
60
50
40
30
20
10
0

FIGURE 16

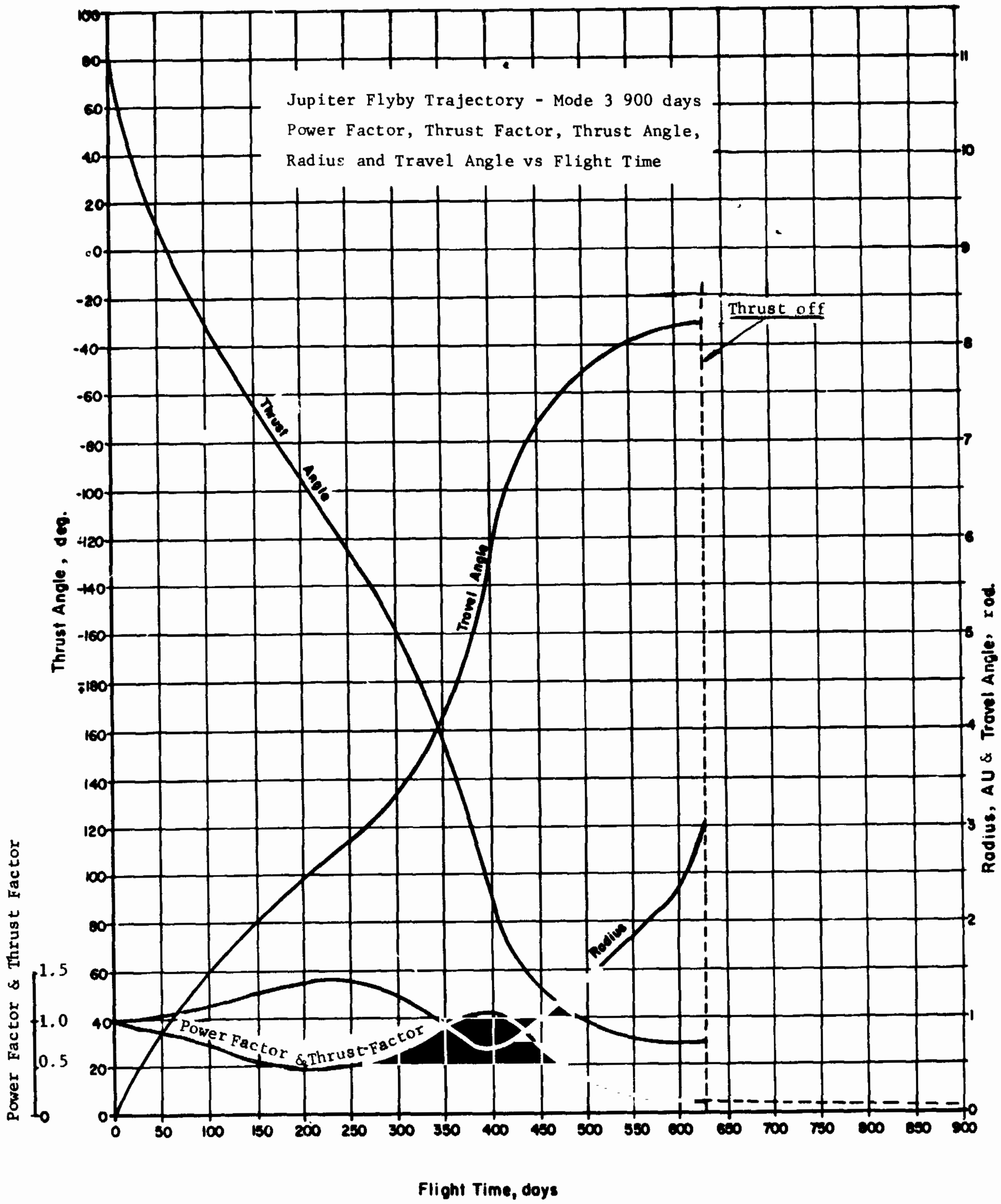
Jupiter Flyby Trajectory - Mode 3 900 days
Power Factor, Thrust Factor, Thrust Angle,
Radius and Travel Angle vs Flight Time
Thrust off
Thrust Angle
Travel Angle
Radius
Power Factor & Thrust Factor
Thrust Angle, deg.
Radius, AU & Travel Angle, rad.
Power Factor & Thrust Factor
Flight Time, days

FIGURE 17

Jupiter Flyby Trajectory - Mode 1
Payload vs Hyperbolic Excess Velocity for
Various Flight Times

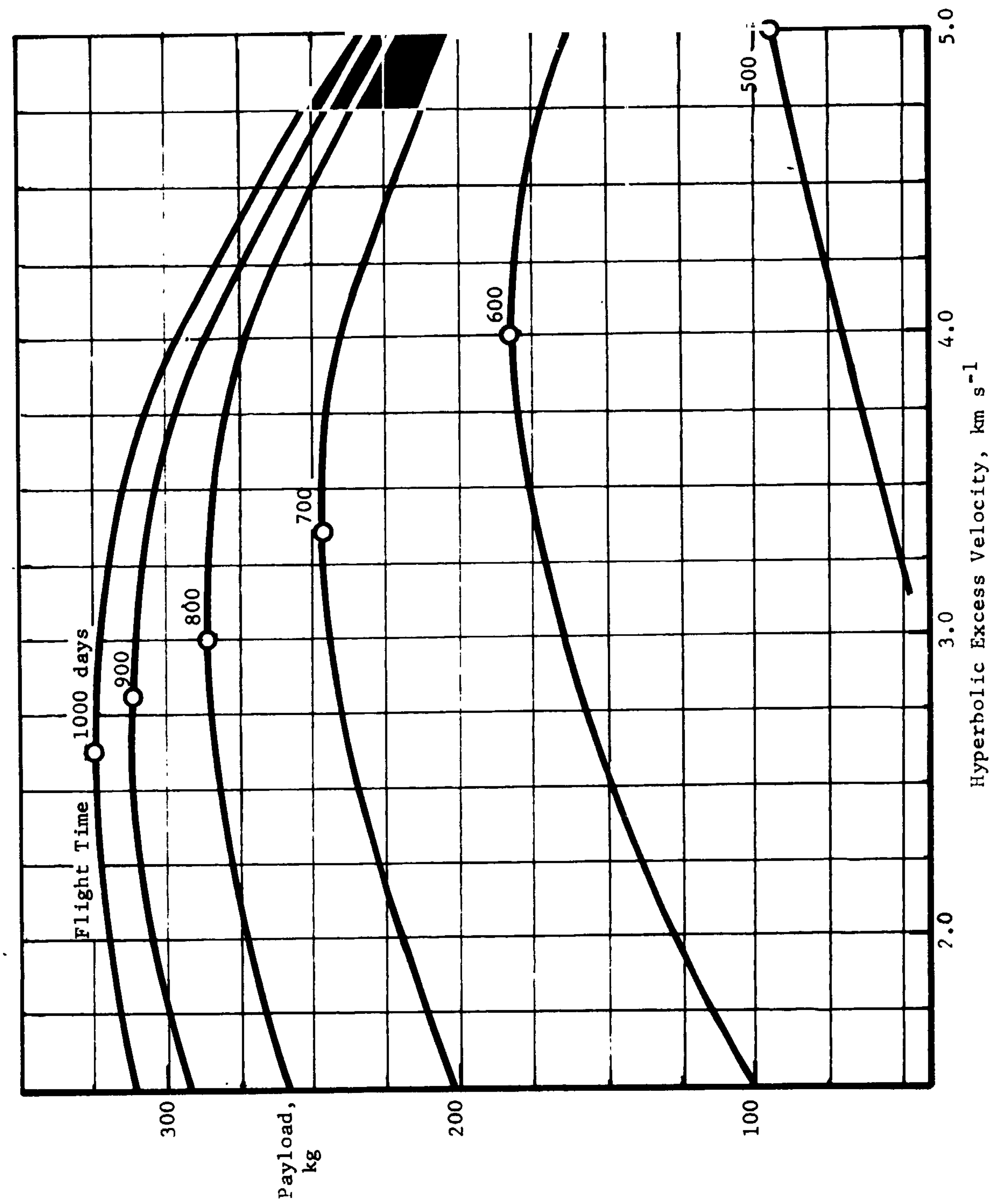

FIGURE 18

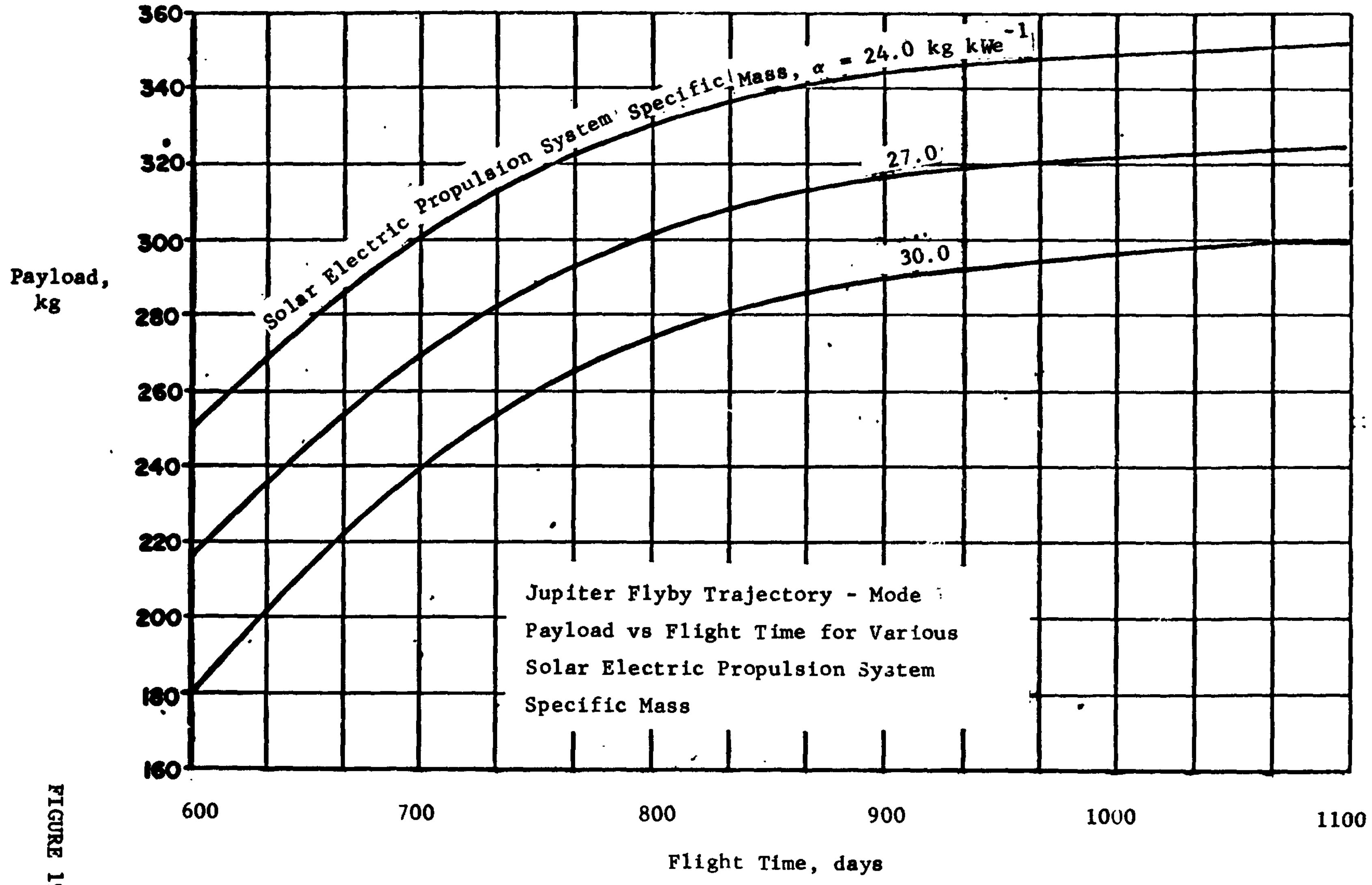
Solar Electric Propulsion System Specific Mass, α = 24.0 kg kWe^{-1}
27.0
30.0
Jupiter Flyby Trajectory - Mode
Payload vs Flight Time for Various
Solar Electric Propulsion System
Specific Mass
Payload, kg
360
340
320
300
280
260
240
220
200
180
160
600
700
800
900
1000
1100
Flight Time, days

FIGURE 19

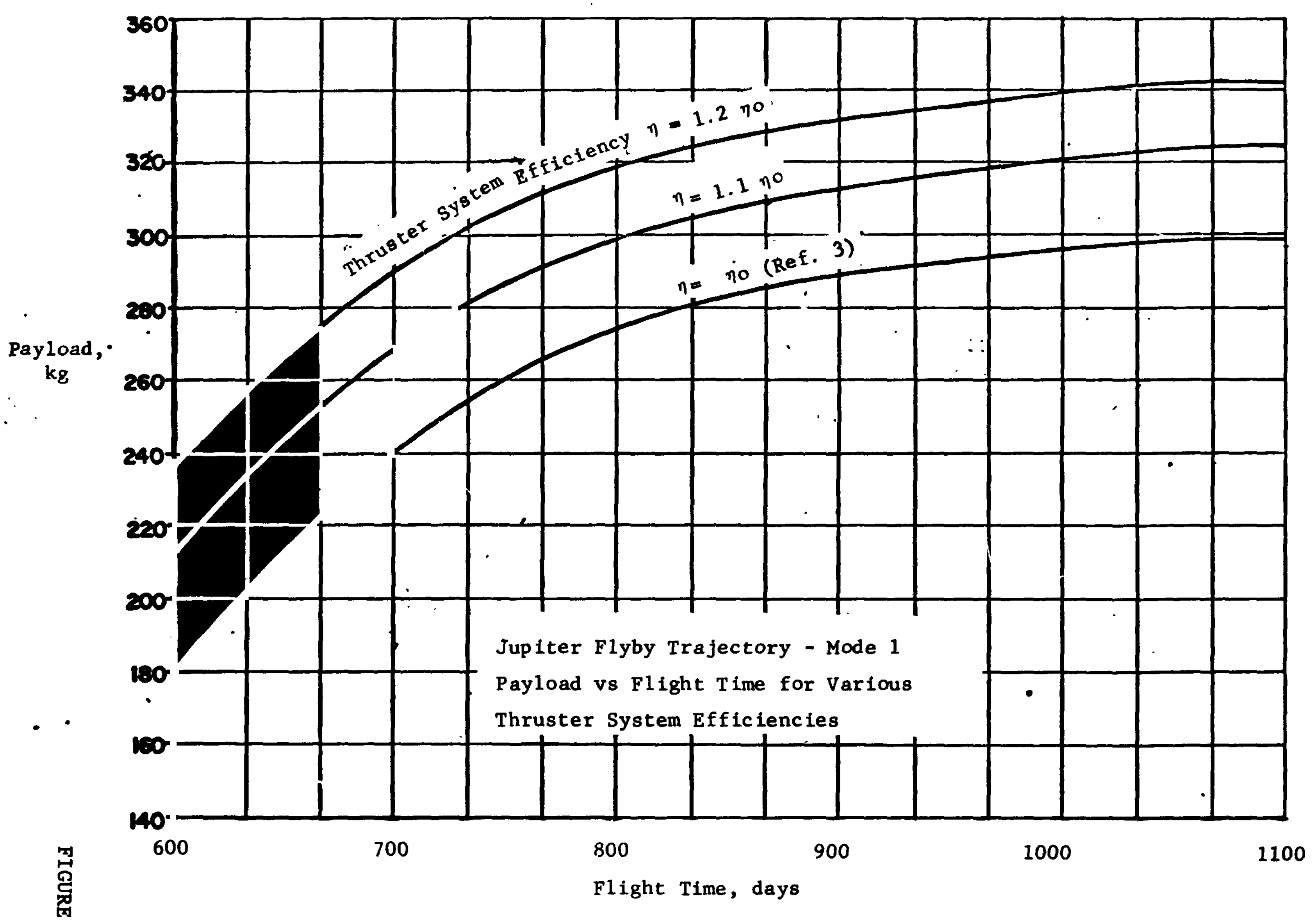
Payload, kg
360
340
320
300
280
260
240
220
200
180
160
140
600
700
800
900
1000
1100
Flight Time, days
Thruster System Efficiency η = 1.2 ηo
η = 1.1 ηo
η = ηo (Ref. 3)
Jupiter Flyby Trajectory - Mode 1
Payload vs Flight Time for Various
Thruster System Efficiencies

FIGURE 20

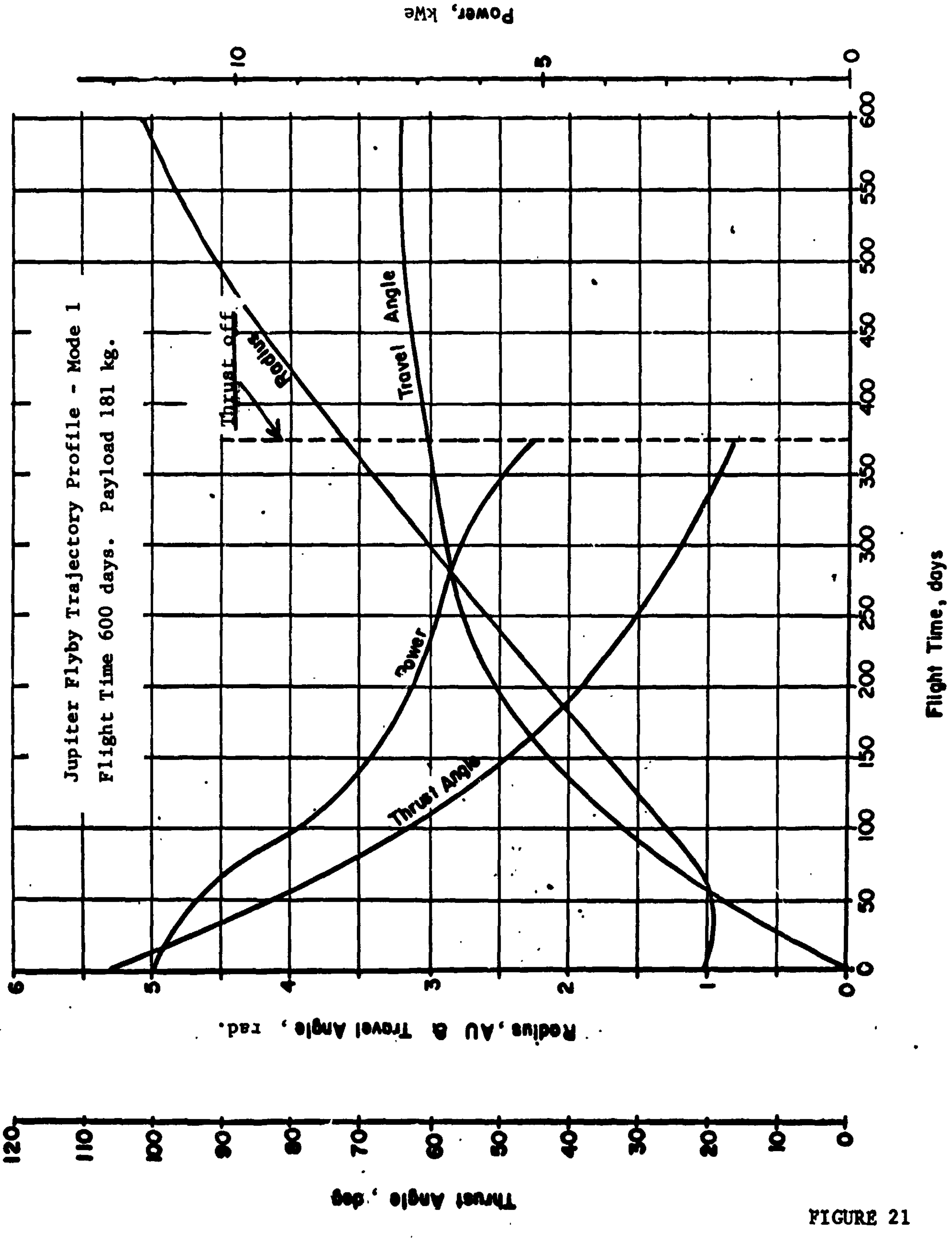
Jupiter Flyby Trajectory Profile - Mode 1
Flight Time 600 days. Payload 181 kg.
Thrust off
Radius
Travel Angle
Power
Thrust Angle
Power, kWe
0
5
10
Flight Time, days
0
50
100
150
200
250
300
350
400
450
500
550
600
Radius, AU & Travel Angle, rad.
0
1
2
3
4
5
6
Thrust Angle, deg
0
10
20
30
40
50
60
70
80
90
100
110
120

FIGURE 21

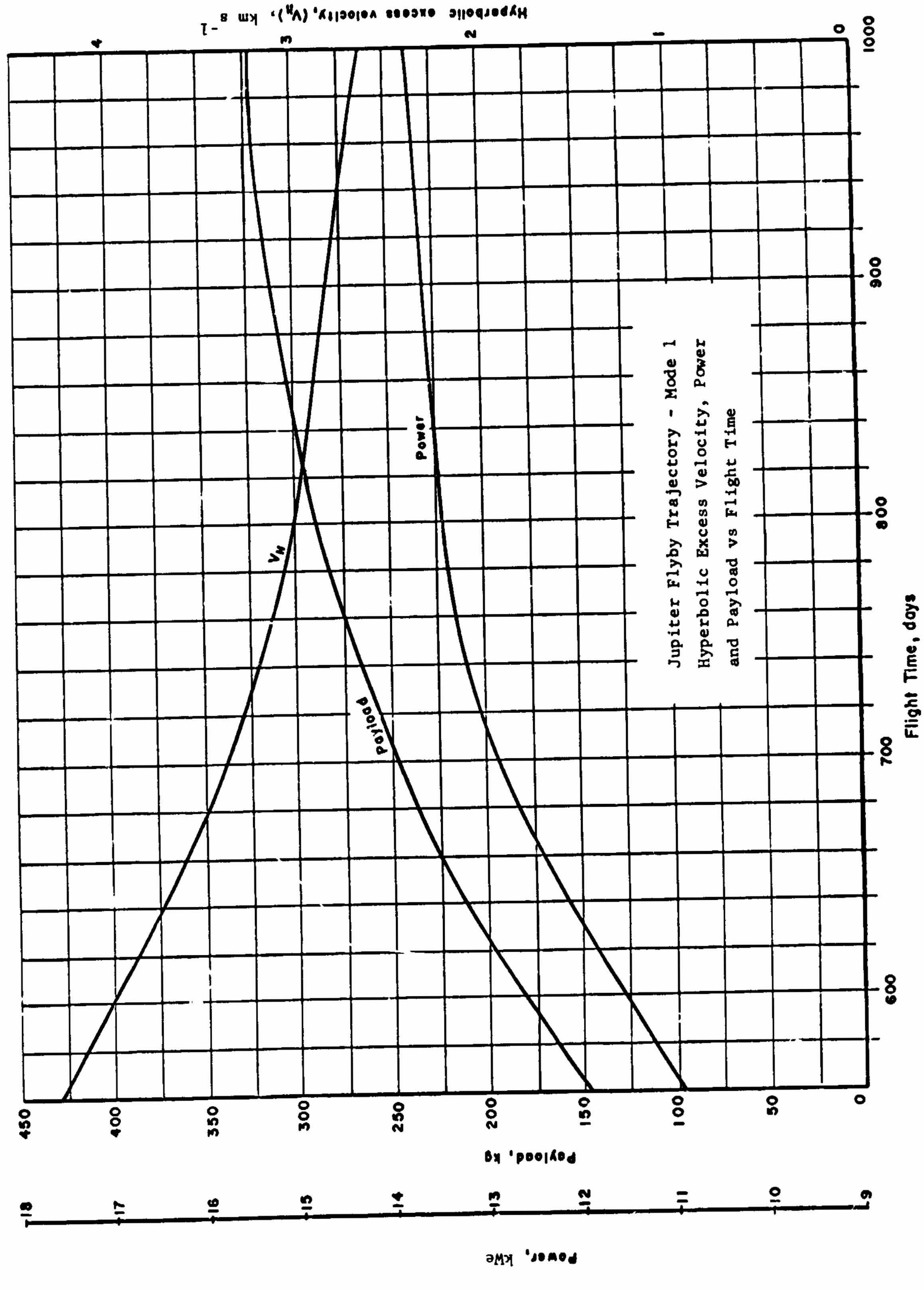
Jupiter Flyby Trajectory - Mode 1
Hyperbolic Excess Velocity, Power
and Payload vs Flight Time
Flight Time, days
Payload, kg
Power, kWe
Power
Payload
V_H
600
700
800
900
1000
450
400
350
300
250
200
150
100
50
0
18
17
16
15
14
13
12
11
10
9
4
3
2
1
0

FIGURE 22

The other trajectory chosen for study was a Mode 3, 900 day flight with payload of about 355 kg. The plot of a similar trajectory is shown in Figure 11 and the actual trajectory profile in Figure 23. Sensitivity of the payload to power, effective jet velocity and hyperbolic excess velocity is shown in Figure 24.

Referring to the sharp falloff of payload with power variation seen in Figures 22 and 24, it should be noted that both effective jet velocity and hyperbolic excess velocity (and thus initial mass) were held constant while the power was varied. Therefore, varying power is essentially the same as varying initial thrust to mass ratio. Previous studies at Princeton have shown also that the payload was quite sensitive to this parameter. If effective jet velocity and hyperbolic excess velocity had been re-optimized for each new power level as has been done in a number of previously studies, the falloff of payload with power would be more gradual and the curve would lie above that shown in Figures 22 and 24.

An interesting comparison of the capabilities of three launch vehicles was made using the Gordon Program: Atlas (SLV3C)/Centaur, Titan III-C(1207)/Centaur and Saturn IB/Centaur. The results are shown in Table 6 below. The mission is a 600 day, solar electric, Jupiter flyby, assuming coplanar circular orbits. The trajectories are fully optimized: thrusting program, effective jet velocity, initial acceleration, power and hyperbolic excess velocity. Transfer angle has also been optimized. The resulting payloads are:

Atlas (SLV3C)/Centaur	174.86 kg
Titan III-C(1207)/Centaur	1943.39 kg
Saturn IB/Centaur	1778.50 kg

The specific mass of the powerplant was taken to be 26.0 kg kWe^{-1}. Tankage and structure factor were assumed to be .06 and .08, respectively.

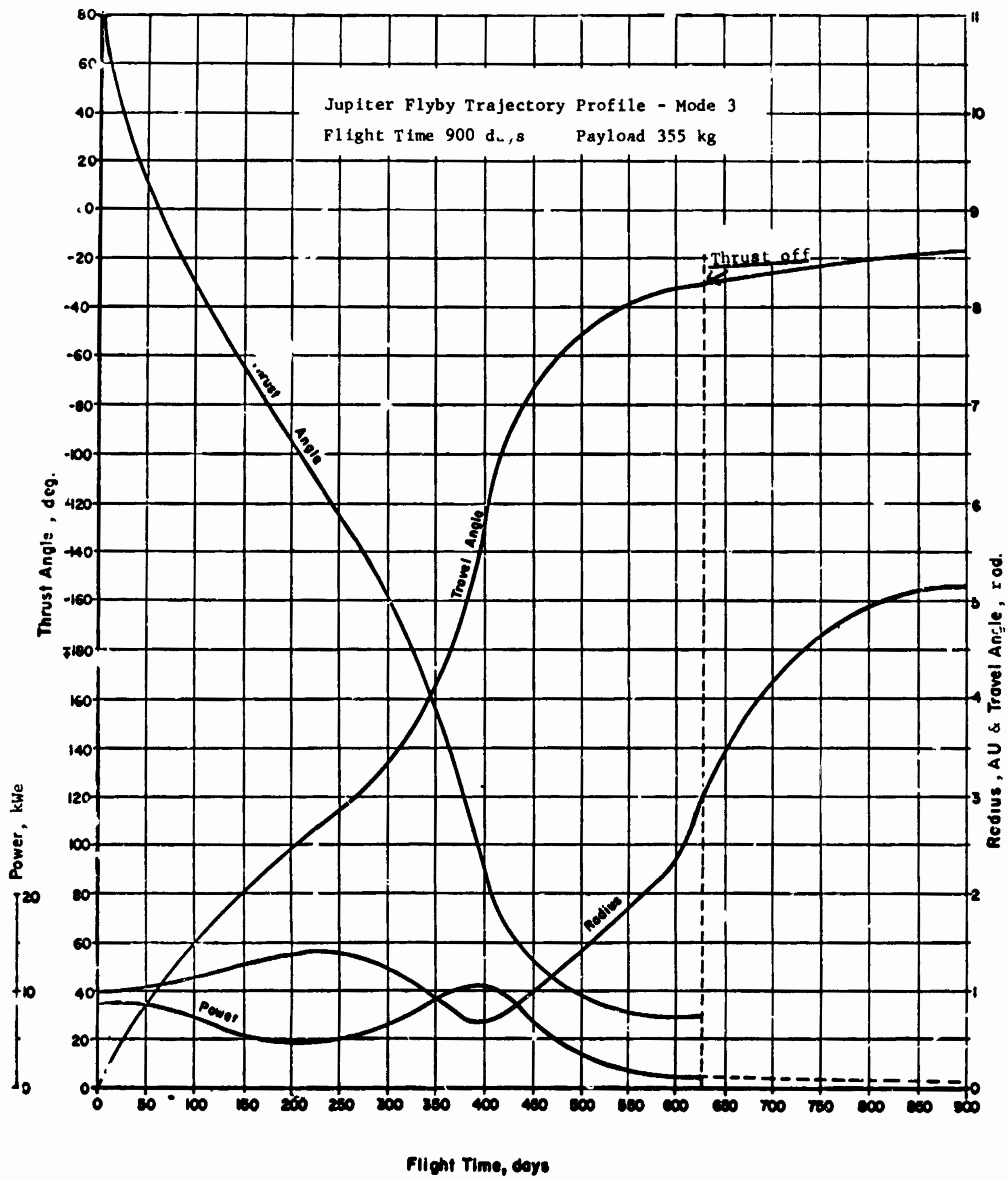
Jupiter Flyby Trajectory Profile - Mode 3
Flight Time 900 d.,s Payload 355 kg
Thrust off
Thrust Angle
Travel Angle
Radius
Power
Thrust Angle, deg.
Power, kWe
Radius, AU & Travel Angle, rad.
Flight Time, days

FIGURE 23

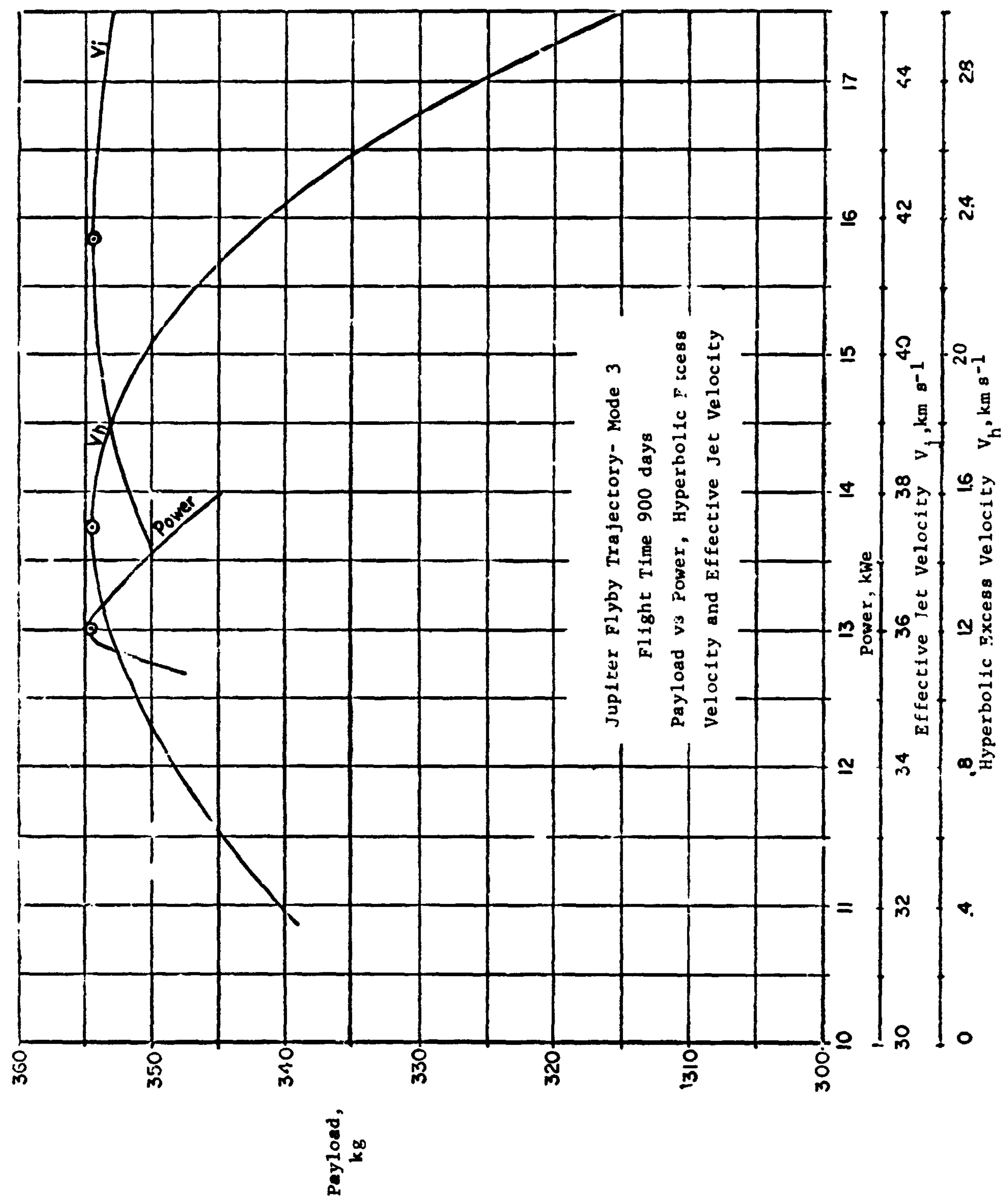
Jupiter Flyby Trajectory- Mode 3
Flight Time 900 days
Payload vs Power, Hyperbolic Excess Velocity and Effective Jet Velocity
Payload, kg
360
350
340
330
320
310
300
Power, kWe
10
11
12
13
14
15
16
17
Effective Jet Velocity Vj, km s-1
30
32
34
36
38
40
42
44
Hyperbolic Excess Velocity Vh, km s-1
0
4
8
12
16
20
24
28
Vj
Vh
Power

FIGURE 24

Table 6

Launch Vehicle Comparison - Jupiter Flyby

Mode 1 - Flight Time 600 days

	Atlas SLV3C /Centaur	Titan III-C (1207) /Centaur	Saturn 1B /Centaur
Initial Mass, kg	696.21	3563.62	3485.39
Powerplant, kg	303.32	913.30	972.72
Propellant, kg	153.15	397.96	429.52
Propellant Tanks, kg	9.19	23.88	25.77
Structure, kg	55.70	285.09	278.83
Payload, kg	174.86	1943.39	1778.50
Initial Power, kWe	11.67	35.13	37.41
Efficiency, η	0.54	0.55	0.54
Hyperbolic Excess Velocity, km s^{-1}	4.03	6.92	6.62
Effective Jet Velocity, km s^{-1}	32.532	32.836	32.805
Initial Acceleration, m s^{-1}	0.5583×10^{-3}	0.3272×10^{-3}	0.3565×10^{-3}

IV. ASTEROID BELT EXPLORATION MISSIONS

A. Introduction

The interest in and value of scientific missions to explore the asteroid belt has been discussed in a number of published papers and reports.[4-10] In addition to scientific interest in the asteroids per se, there is also the need to know more about the asteroids from the viewpoint of collision - avoidance between the asteroids and any interplanetary spacecraft passing through the belt as well as the contribution of the asteroids to the dangerous-sized particles and debris throughout the rest of the solar system.[11-15] An asteroid belt fly-through mission is examined in Refs. 4 and 5. Four rendezvous missions to the asteroids Eros, Ceres, Icarus, and Vesta, respectively, are examined in Ref. 5. Since all of these mission studies are based upon chemical propulsion, it was decided to make some preliminary analyses based on solar electric rocket propulsion.

B. Discussion of Solar-Electric Asteroid Belt Trajectory Results

The feasibility of optimal rendezvous trajectories to targets within the asteroid belt, using a solar-electric propelled spacecraft, launched by one of three designated boosters [Atlas (SLV3C)/Centaur, Titan III-C(1207)/Centaur, or Saturn 1B/Centaur] was initially reported in ASMAR Status Report dated 1 October 1967.[16] A more complete set of data is presented and summarized in this report.

The general pattern of the asteroid rendezvous trajectories is shown in the FRONTISPIECE.

Figures 25, 26, 27 and 28 show curves of payload m_{pl}, initial solar electric power at 1 AU P_o, hyperbolic excess velocity squared C_3, and effective

Solar Electric Propelled Asteroid Rendezvous
at R = 2.0 AU

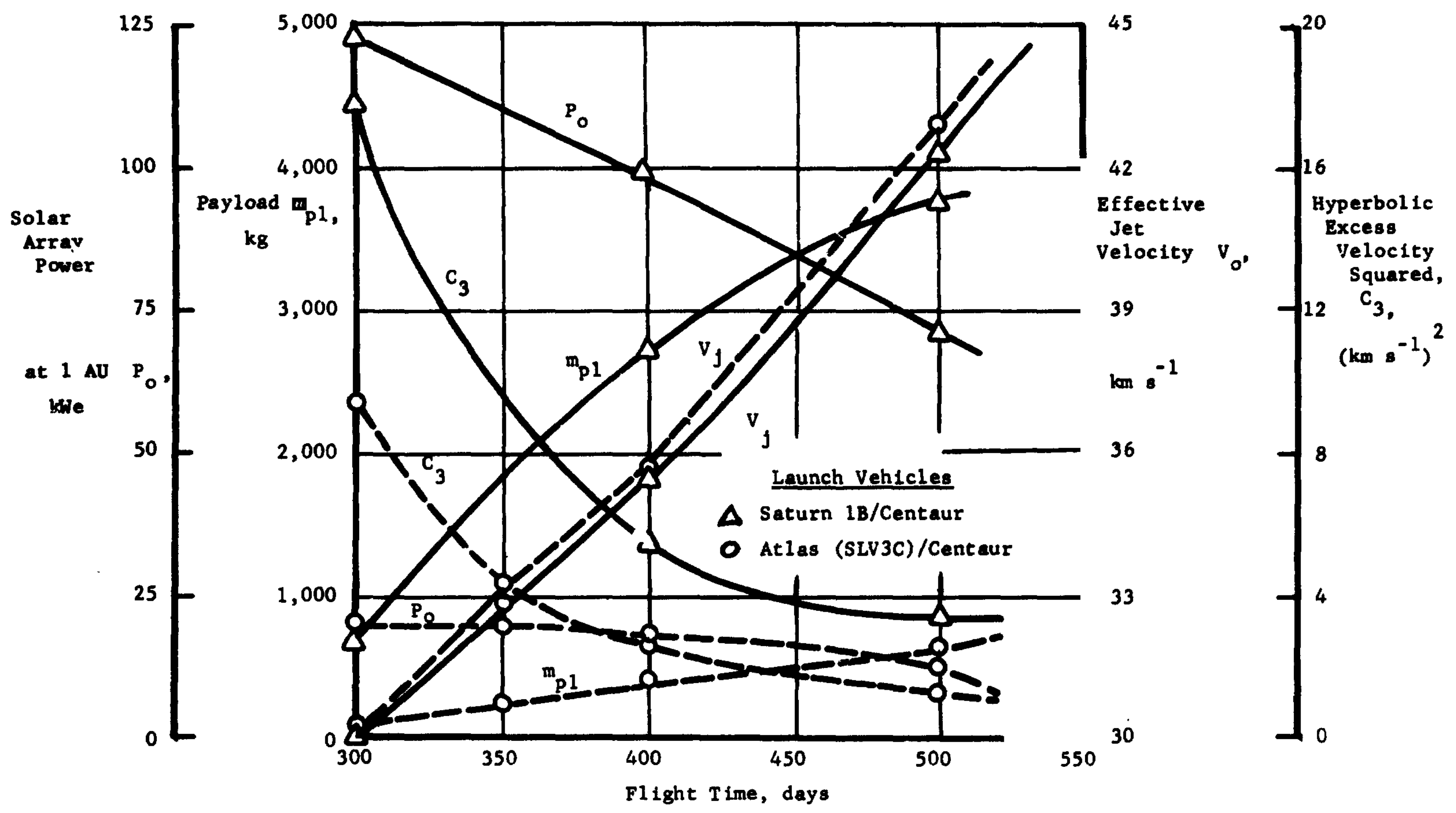

FIGURE 25

Solar Electric Propelled Asteroid Rendezvous
at R = 3.0 AU

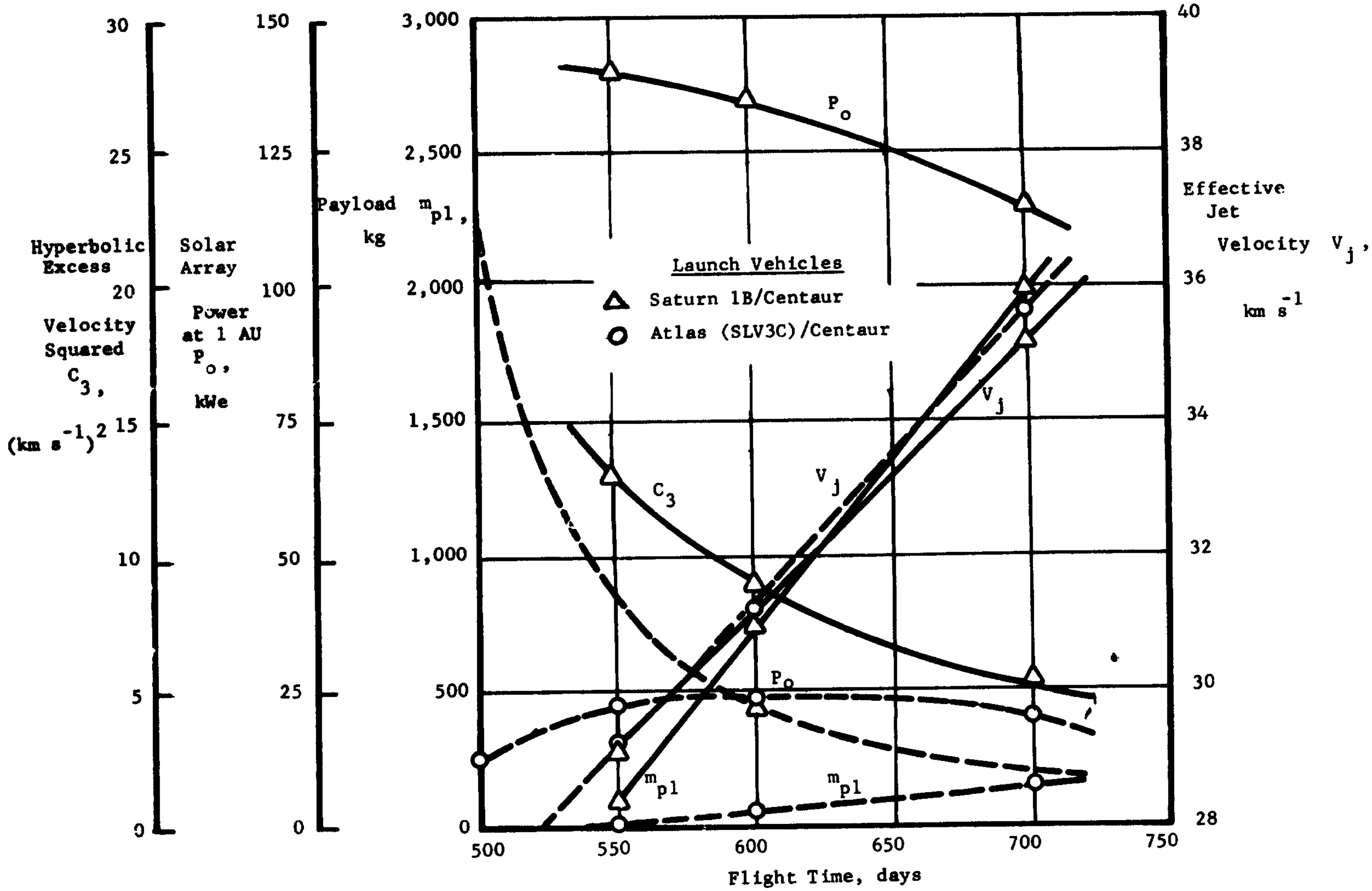

FIGURE 26

Solar Electric Propelled Asteroid Rendezvous
at R = 3.5 AU

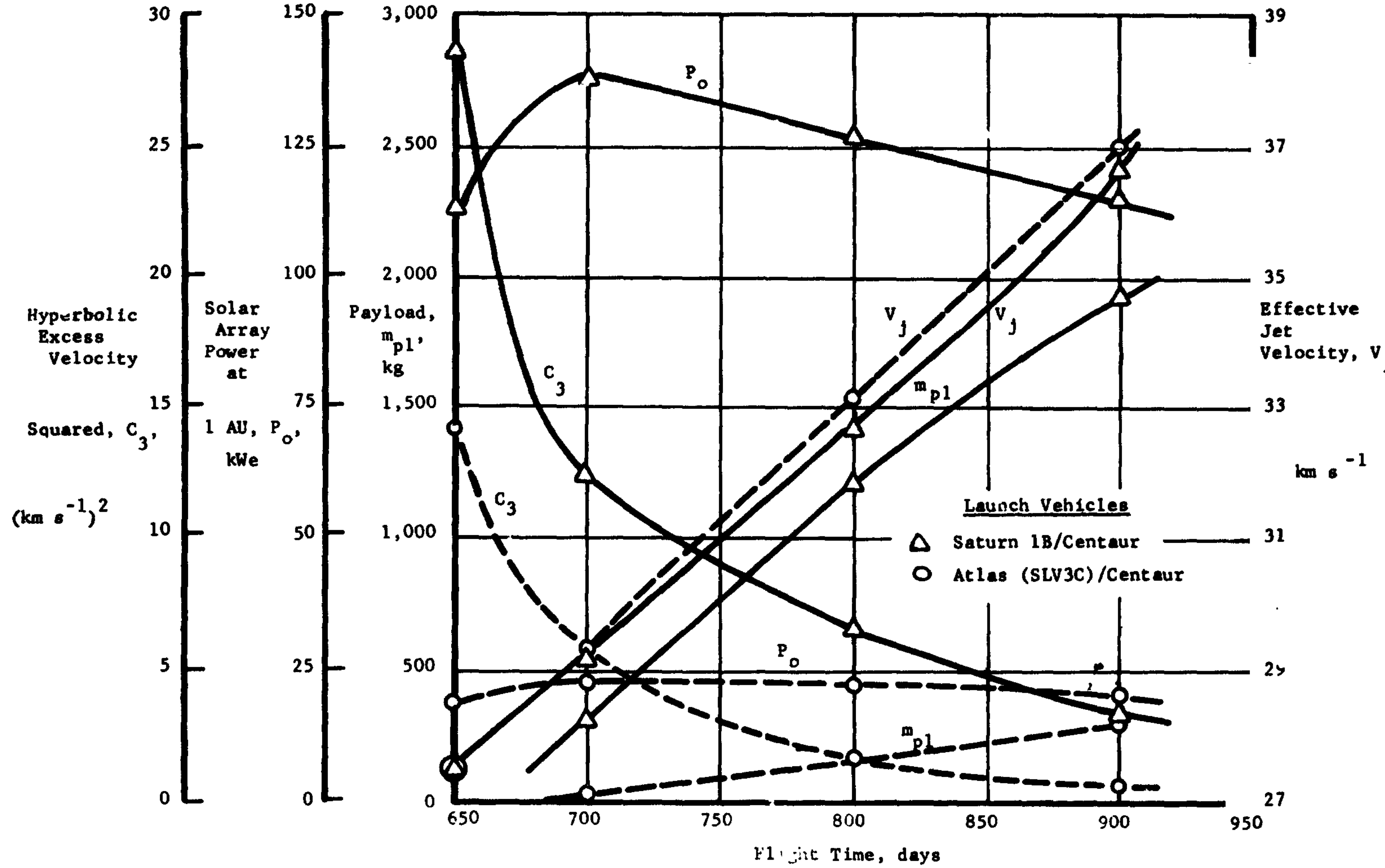

FIGURE 27

Solar Electric Propelled Asteroid Rendezvous
at R = 4.0 AU

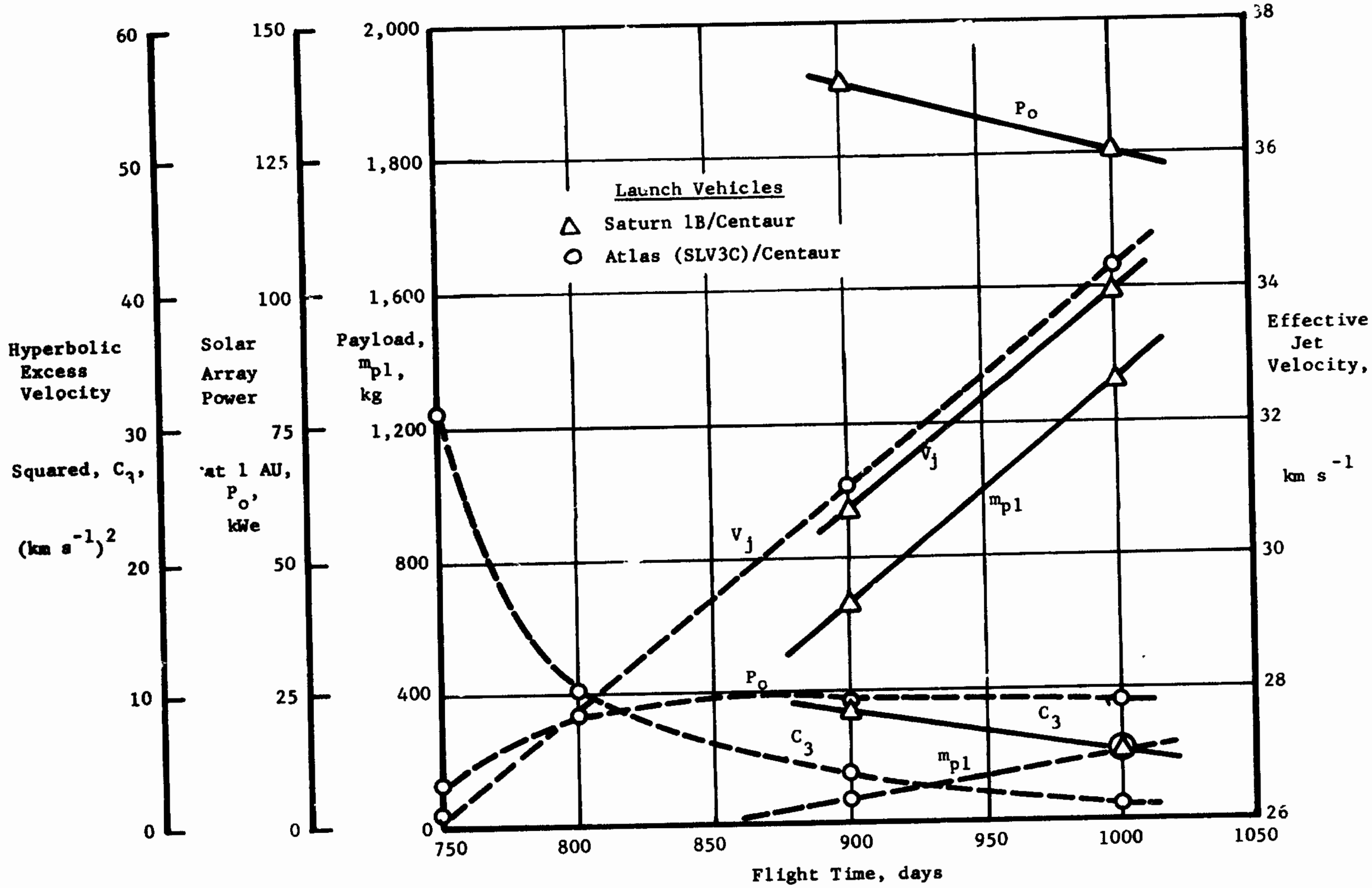

FIGURE 28

jet velocity V_j vs flight time for the Atlas (SLV3C)/Centaur and the Saturn 1B/Centaur boosters, for rendezvous missions to radii R = 2.0, 3.0, 3.5 and 4.0 AU, which includes the approximate radial extent of the asteroid belt. This data is also presented in tabular form in Table 7. These trajectories are fixed-time, two-dimensional optimized for maximum payload with respect to the thrust program, P_o, V_j, C_3 and travel angle. The following quantities are input data: electric rocket propulsion system specific mass factor α = 20.0 kg kWe^{-1}, (44 lbs/kWe), structure factor = 0.08, tankage factor = 0.06, thruster system efficiency η = a function of V_j (Figure 7), the solar power fall-off function = a function of solar distance R (Figure 8), and the launch vehicle characteristics.[2] The specific mass factor is considered to be representative of advanced solar array technology in the period when these missions would be performed. These are rendezvous trajectories, which match the local heliocentric circular orbital velocity at each designated radius, R. Thus the trajectory matches the orbit of the average asteroid, assumed circular. Match to prescribed elliptical orbits is easily obtainable, if desired. Since the asteroids are closely grouped about the ecliptic plane, there is not expected to be a significant change in payload performance between these two-dimensional (ecliptic plane) trajectories and actual three-dimensional ones. The justification for this statement is that it is known that for small orbital inclination angles, which is the case here, there is only a small payload performance penalty for non-coplanarity, using electric propulsion on interplanetary trajectories.[15]

Figures 25 through 28 and Table 7 show clearly, assuming a minimum payload limit of about 340 kg (750 lbs), that rendezvous missions within the entire asteroid belt are feasible using the Saturn 1B/Centaur booster and solar electric propulsion. The payload masses, while function of the trip time as

Table 7

Solar Electric Asteroid Rendezvous

Final Radius	Time	Net (Final less Powerplant) Mass	Electric Power at 1 AU P_o	Final Electric Power P_f	Jet Exhaust Velocity V_j	Electric Engine Efficiency	C_3	Travel Angle	Payload Mass
AU	days	kg	kWe	kWe	km s^{-1}	%	$(km\ s^{-1})^2$	rad	kg
Saturn 1B/Centaur Plus Solar Electric									
2.0	300	1245	123.6	37.7	30.0	60	17.8	2.66	695
	400	3310	99.2	30.0	35.4	66	5.6	3.60	2710
	500	4365	70.9	21.6	42.5	73	3.4	4.48	3750
3.0	550	840	140.0	19.1	29.1	58	13.0	3.26	188
	600	1505	135.0	18.4	31.0	61	8.9	3.57	881
	700	2560	114.4	15.6	35.2	66	5.4	4.16	1921
3.5	650	385	113.2	11.5	27.5	56	28.8	3.14	0
	700	900	138.7	14.1	29.2	59	12.5	3.50	313
	800	1870	128.8	13.1	32.7	63	6.6	4.03	1227
	900	2595	115.0	11.7	36.7	68	3.4	4.59	1927
4.0	900	1300	137.0	10.8	30.7	61	8.5	3.91	663
	1000	2010	125.4	10.0	33.9	65	5.2	4.36	1337
Atlas (SLV3C)/Centaur Plus Solar Electric									
2.0	300	170	21.3	6.5	30.0	60	9.4	2.73	78
	350	370	20.8	6.3	32.8	64	4.3	3.22	268
	400	530	17.7	5.4	35.7	67	2.7	3.68	425
	500	720	12.9	3.9	42.9	73	1.3	4.60	610
3.0	500	20	12.8	1.8	27.0	55	23.6	2.92	0
	550	120	22.1	3.0	29.2	59	8.6	3.32	20
	600	230	23.5	3.2	31.2	61	4.1	3.67	122
	700	415	20.3	2.8	35.6	67	2.0	4.30	300
3.5	650	45	18.7	1.9	27.5	56	14.3	3.27	0
	700	130	23.5	2.4	29.3	59	6.3	3.60	27
	800	300	23.1	2.4	33.1	64	2.0	4.19	185
	900	425	20.0	2.0	37.0	68	1.3	4.71	310
4.0	750	5	8.2	0.65	26.1	54	31.1	3.13	0
	800	60	21.4	1.7	27.7	56	10.2	3.51	0
	900	200	23.4	1.9	30.9	61	4.1	4.02	90
	1000	325	22.4	1.8	34.3	65	1.3	4.55	208

Optimal Thrust, V_j, C_3, P_o. Structure Factor = 0.08 α = 20.0 kg kWe^{-1}
Tankage Factor = 0.06

shown, remain amply adequate in most cases for a wide spectrum of experiments, communication capabilities, terminal maneuvers, cruising among a number of locations within the asteroid belt, orbiting around or surface-landing upon an asteroid, etc. A detailed examination of such experiments and terminal maneuvers, while of considerable interest and importance, was beyond the planned scope of this work, and has not been performed. The Atlas (SLV3C)/Centaur booster plus solar electric propulsion appears adequate (based upon the 340 kg minimum payload limit) at R = 2.0 AU for trip times greater than about 400 days, not adequate at R = 3.0 AU for trip times less than 700 days, marginally adequate at R = 3.5 AU for trip times greater than about 950 days and not adequate at R = 4.0 AU for trip times less than 1,000 days. Thus, it appears that the Atlas (SLV3C)/Centaur booster plus solar electric propulsion is marginally suitable for rendezvous missions to regions within the asteroid belt up to about R = 3.5 AU, depending upon the maximum allowable flight time and the minimum allowable payload mass.

It must be kept in mind that the solar-electric powerplant masses are not included in the above payloads. This is an important point when making comparisons with non-electric propelled systems, which require separate sources of electric power, and which are usually charged against the payload mass. On the other hand, the optimum power levels are in some instances larger than practicable with certain constraints such as shrouds, etc.

The electric power available at the trajectory terminals is listed under the heading P_f in Table 7. The power at any distance R is given by the usual equation

$$P_f = P_o \, f(R) \qquad (1)$$

where P_o is the initial power at 1 AU and f(R) is the prescribed variation of power with solar distance R. For the Saturn 1B/Centaur, the terminal power P_f exceeds 10 kWe in all cases. This power level (10 kWe) at S-band (2300 MHz), using a spacecraft antenna diameter of 7.5 feet, should be adequate for most communication needs, and can provide a bit rate of 20,000 bits/sec at 5.0 AU range to Earth, using the 85 foot DSIF ground antenna.[5] This power level (10 Kw) is also adequate for the larger of two experimental radars mentioned in the following section of this report. The desirability of a television capability, not necessarily real-time, implies that high data rates will be required at ranges up to 5.0 AU. For real-time television, using Apollo television parameters, FM modulation, 5.0 AU range, 85 foot ground antenna, 7.5 foot spacecraft antenna, 160 kWe of power would be required. This would be reduced to 30 kWe by use of an 18 foot spacecraft antenna.

The circularized rendezvous trajectories discussed above comprise only one subclass of the total number of potentially useful trajectories to explore the asteroids. For example, another subclass of rendezvous trajectories are rendezvous missions to specific named asteroids, with known orbital elements. Still other types of trajectories, such as a "cruiser" or spiraling trajectory may provide better sampling of the total asteroid distribution within the belt, if this is the scientific mission objective, in radius (solar distance), in angle (circumsolar) and in depth (direction normal to ecliptic plane) than rendezvous trajectories. Such missions may accomplish more per mission dollar measured in terms of data-gathering and in accumulation of scientific knowledge than rendezvous trajectories. Of course, it may be possible to design rendezvous trajectories which provide a good sampling of the belt prior to or even subsequent to rendezvous with a specific asteroid, if sufficient propulsion capability is available.

Another trajectory subclass is the flyby or fly-through type of mission which can deliver more payload than the rendezvous type, but also has disadvantages, as will be discussed now. Two examples of fly-by or fly-through trajectories were investigated briefly. The results are tabulated in Tables 8 and 9. The first trajectory type (labeled Type 1, Table 8) consists of a 450-day trip to R = 4.0 AU. Optimal thrust is used to R = 2.0 AU, then thrust is cut off, and the vehicle coasts to 4.0 AU. The trajectory goes on beyond 4.0 AU but was not computed. This trajectory has the following advantage over the rendezvous types: A solar distance of 4.0 AU (spanning the belt) is reached in only 450 days, which trip time is not achievable at all, with any of the designated boosters, for the circular-orbit rendezvous type trajectory to R = 4.0 AU, and this with payloads comparable to those of the circular-orbit rendezvous type at R = 2.0 AU. However, there are corresponding disadvantages, such as a smaller travel angle (poorer circumsolar sampling) and faster transit time through the belt (increased experiment observational difficulties) compared with the open-angle circular-orbit rendezvous trajectories. For example, for the Saturn 1B/Centaur, comparison between the above 450 day Type 1 trajectory, and the 900-day circular-orbit rendezvous trajectory shows that the travel angle and time within the belt (~2 to 4 AU) for the latter are respectively each approximately twice that of the former. This is shown in Table 8.

It can be seen from Table 8 that the performance of the Titan III-C (1207)/Centaur and the Saturn 1B/Centaur boosters are very similar to each other. Partly for this reason an extensive separate set of trajectory computations using the Titan booster was not undertaken. Another comment on Table 8 (and 9) is that a powerplant specific mass factor of α = 26.0 kg kWe^{-1} was used instead of 20.0 kg kWe^{-1} used for Table 7, due to the computation being done at two different time periods. While this difference in α can produce

Table 8

Solar Electric Asteroid Fly-Through Trajectory Type 1*

	Saturn 1B /Centaur	Titan III C (1207)/Centaur
Initial Power, P_o, kWe	31.2	27.7
Effective Jet Velocity, V_j, km s^{-1}	31.4	31.4
Hyperbolic Excess Velocity Squared, C_3, $(km\ s^{-1})^2$	44.1	48.4
Initial Thrust Accel., FMO, m s^{-2}	0.30×10^{-3}	0.26×10^{-3}
Initial Mass, m_o, kg	3,475	3,530
Engine Efficiency, η	0.53	0.53
Payload Mass, m_{pl}, kg	2,085	2,270

	Saturn 1B /Centaur		Titan III C (1207) /Centaur	
Time, days	Distance, AU	Travel Angle, rad.	Distance, AU	Travel Angle, rad.
0	1.00	0	1.00	0
75	1.34	1.32	1.36	1.31
150	2.00	1.99	2.00	1.93
300	3.14	2.49	3.16	2.46
450	4.00	2.75	4.00	2.73
	within belt (~2-4 AU): time = 300 days angle = 0.76 rad.		within belt (~2-4 AU): time = 300 days angle = 0.8 rad.	

For comparison: Saturn 1B/Centaur, 900-day, 4.0 AU rendezvous: within belt: time = 700 days, angle = 1.7 rad.

*Type 1 trajectory: 450 days to R = 4.0 AU. Optimal thrust control to R = 2.0 AU, coast to 4.0 AU. α = 26.0 kg kWe^{-1}, tankage factor = 0.06, structure factor = 0.08.

2

Table 9

Solar Electric Asteroid Fly-Through Trajectory Type 2*

Titan III-C(1207)/Centaur

Initial power, P_o, kWe	53.3
Jet exhaust velocity, V_j, km s^{-1}	31.4
Hyperbolic Excess Velocity Squared, C_3, (km $s^{-1})^2$	53.7
Initial thrust accel., FMO, m s^{-2}	0.30×10^{-3}
Initial mass, M_o, kg	3,240
Engine efficiency, η	0.53
Payload mass, m_{pl}, kg	850

Time, days	Distance, AU	Travel Angle, rad.	Mass, Normalized
0	1.00	0	1.00
125	2.00	1.61	0.88
250	3.00	2.02	0.84
435	4.00	2.30	0.81
700	4.50	2.54	0.78

Within belt (~2-4 AU), outward-bound leg:
Time = 310 days
Angle = 0.69 rad.

*Type 2 trajectory: 700 days to R = 4.5 AU. Optimal continuous thrust. Terminal velocity = 0, tangential velocity open and less than local circular velocity, so that spacecraft falls back into belt.

meaningful differences in payload, it is not large enough to invalidate the overall remarks on comparative performance between rendezvous and nonrendezvous subclasses of trajectories made in the preceeding paragraph.

The second type of trajectory (labeled Type 2, Table 9) consists of a 700 day trip to R = 4.5 AU, optimal continuous thrust, terminal radial velocity = 0 and terminal horizontal velocity = open, but less than local circular velocity at R = 4.5 AU, so that the spacecraft falls back into the belt. The results (Table 9) are not very promising, as compared to previous trajectories, in terms of payload, and time and angle spent within the belt on the outbound leg. A possible significant improvement might be achieved by shortening the trip time somewhat by reducing the radius to R = 4.0 AU, and by including the return (inbound) leg contributions to the time and angle within the belt.

A very novel possibility is a solar-electric mission to accomplish a complete 360° sampling in circumsolar angle in the belt in a reasonable time by use of a retrograde solar orbit. It is proposed to establish such an orbit by means of a Jupiter swing-by, to put the spacecraft into a retrograde circular or elliptic orbit within the belt. One disadvantage of such a trajectory would be the very high relative velocities between the asteroids in their posigrade orbits and the spacecraft in its retrograde orbit. More study is needed to establish trajectory feasibility, and to assess the aggravated experimental difficulties due to the high spacecraft velocity relative to the asteroids.

C. Spacecraft Radar

The desirability of an on-board radar for detection, range, angle and other possible measurements on asteroids in a program aimed at exploration of the belt is discussed in the literature.[4,5] In addition, some type of radar is required to furnish input data for asteroid collision avoidance systems.[11,12,13] For exploration, the radar would need to be supplemented by other equipment for detailed measurements of asteroid size, orbital elements, rotation, and surface characteristics. For collision avoidance, additional subsystems would be needed for asteroid target tracking, trajectory prediction, and maneuverability command and control.

A study of the feasibility of such a radar was completed, and is reported in detail in Ref. 18, and in summary form in Ref. 16. Sincc Ref. 18 is an available and self-contained report, there is no need to repeat details at length in this final report. It is concluded in Ref. 18 that some type of radar will be both useful and feasible assuming continued development of the state-of-the-art into the 1970's. There is presently a problem in estimating the radar capabilities. As an exploration tool, the value of the radar would be measured by the number of detected asteroids. Any estimate of this number depends upon an assumed asteroid distribution in number, size and velocity in the belt. At present, this distribution is completely unknown, except for the largest asteroids, which comprise, it is thought, a very small fraction of the total. Hence the calculated radar usefulness varies by several orders of magnitude, depending upon the assumed distribution. Two radars and various scan modes are examined, a smaller one at 0.1 kWe and a larger one at 10 kWe average power, using an up-to-date asteroid distribution.

V. CONCLUSION WITH RECOMMENDATIONS

The work presented in this report must be considered to be preliminary and exploratory in nature from the standpoint of fully optimized missions. However, the results do attest to a considerable capability for broad optimization of solar electric propelled spacecraft trajectories recognizing constraints related to realistic modelling of flight paths in the solar system using actual planetary ephemerides. Further development of trajectory analysis capability is recommended to understand more fully the interactions between realistic trajectories, available spacecraft technologies and actual mission performance with solar electric propulsion. The capability for analyzing other more complex and detailed missions should be established without undue delay.

The Mars orbiter 1971-79 checks provided a substantial, although tentative, agreement with the Hughes Aircraft Company trajectories. It is recommended that in the future full record of input data and constraints be retained so that cross checks of the results can be made with definitive accuracy.

The solar electric propelled Jupiter flyby trajectories using the Atlas (SLV3C)/Centaur launch vehicle disclosed several distinct modes and their relative characteristics. The trajectory analysis computer programs were shown to be capable of extensive flexibility in optimizing the mission and in determining the sensitivities among the various parameters. It is recommended that further and improved analyses of Jupiter flybys and swingbys be undertaken as the definition of mission requirements; i.e. - payloads, flight times, et al., become more certain and detailed and in the light of technology advances. Launch vehicle, especially Titan family and newer booster, characteristics and costs will be of considerable importance and must be factored into the analyses.

Asteroid missions are shown to be interesting possibilities for solar powered-electric rocket propelled spacecraft. The asteroid rendezvous missions are particularly suited to solar electric propulsion and the power requirements of the payloads, which may include radars, can probably be well satisfied from the solar array power sources. Other asteroid, planetoid and cometary missions including retrograde flight paths may benefit from the unique characteristics of solar electric propulsion. It is recommended again that the Titan family and other intermediate launch vehicles be studied for their applicability of these missions.

There are many more variables to be exploited in the concepting of spacecraft and their trajectories for missions where solar electric propulsion may be applicable and optimum. It is recommended that attention be given well ahead of the requirement for the analysis of future missions to the development of the needed trajectory analysis capability for use in the concepting of the spacecraft with their payloads. To do this it will be necessary to handle solar system constraints and flight path requirements in realistic and detailed fashion in the trajectory analysis, project the applicable propulsion and other systems technology, and identify the science payloads with their mass, volume and power requirements as part of an ongoing program for solar system exploration.

REFERENCES

1. Hughes Aircraft Company, Solar-Powered Electric Propulsion Spacecraft Study, Jet Propulsion Laboratory Contract No. 95144 (December 1965).

2. NASA Launch Vehicle Estimating Factors for Generating OSSA Prospectus 1967, November 1966.

3. NASA Headquarters (J. P. Mullin) Letter, dated January 19, 1967.

4. Greenspan, J. A., Technology Requirements for Deep Space Measurements, Asteroid Fly-Through Mission, Illinois Institute of Technology Research Institute (IITRI) Report No. S-2, April 1966.

5. Friedlander, A. L. and Vickers, R. S., A Survey of Missions to the Asteroids, IITRI Report No. M-3 (undated).

6. Narin, F., Spatial Distribution and Motion of the Known Asteroids, AIAA Journal Spacecraft & Rockets, Vol. 3, No. 9, September 1966, 1438-1440.

7. Wood, J. A., Meteroites and Asteroids, Advances in the Astronautical Sciences, Vol. 19, Unmanned Exploration of the Solar System, Denver, 1965, American Astronautical Society Publication.

8. Bernstein, R., The Asteroids - A Twenty-Year Survey of the Literature, General Electric Company, Missile and Space Division, Report R64SD19, March 1964.

9. Kohler, G. M., The Importance of Minor Planets in Space Exploration, I.A.F. Meeting, Varna, Bulgaria, September 1962.

10. Moore, G. O. and Jensen R., Comet and Close Approach Asteroid Mission, Advances in the Astronautical Sciences, Vol. 20, Pt. 2, American Astronautical Society Publication, May 1965.

11. Volkoff, J. J., System Protection Requirements for the Resistance of Meteoroid Penetration Damage, AIAA Journal Spacecraft and Rockets, Vol. 3, No. 1, January 1966, 26-34.

12. Marshall, R., Shielding of Jupiter Flyby Spacecraft from Meteoroids, California Institute of Technology, Jet Propulsion Laboratory, Interoffice Memo 2947-69, March 1, 1966.

13. Electronic Systems Requirements Study for Asteroid Collision Avoidance, Exhibit "A", NASA ERC, R&D 67-263.

14. Dixon, W. J., Major System Design Problems for Deep Space Probes, AIAA Paper 66-887.

15. Bender, D. F., Asteroid Encounters on Mars Missions, Space Flight Mechanics Specialist Conference, Denver, Colorado, American Astronautical Society Preprint 66-124, July 1966.

16. Lion, P. M., Aerospace Systems and Mission Analysis Research Status Report for the Period 1 July-30 September 1967, Princeton University, 1 October 1967.

17. Melbourne, W. G., Interplanetary Trajectories and Payload Capabilities of Advanced Propulsion Vehicles, California Institute of Technology, Jet Propulsion Laboratory, Technical Report No. 32-68, March 31, 1961.

18. Handelsman, M., Preliminary Study of Radar Subsystems for Asteroid Belt Exploration Spacecraft, ASAR Memo No. 5, Aerospace Systems and Mission Analysis Research Group, Princeton University, 3 October 1967.